Strange Meson Spectroscopy at Hall D

Volker Credé

Florida State University, Tallahassee, Florida

K_L Meeting

Jefferson Lab

01/18/2017

K_L-Beam in Meson Spectroscopy

VES at Protvino and Crystal Ball at BNL; Other Experiments?

LASS at SLAC: Last experiment to scatter low-momentum (11 GeV/c)
Kaons off protons (in the 1970s)

1 K^* Spectroscopy

VES	Hall D	Photoproduction
$K^- p \to (\bar{K}^0 \pi^+ \pi^-) n$	$K_L p \to (K_S \pi^+ \pi^-) p$	$\gamma p \to K^{*0} \Sigma^+$
$K^- p \to (K^- \pi^+) n$	$K_L p \to (K^- \pi^+) p$	
$K^- p \to (\bar{K}^0 \pi^-) p$	$K_L p \to (K_S \pi^+) n$	
$K^- p \to (K^- \eta) p$	$K_L p \to (K^+ \eta) n$	

2 $s\bar{s}$ Spectroscopy

VES	Hall D	Photoproduction
$K^- p \to (K_S K_S) \Lambda$	$K_L p \to (K_S K_S) \Sigma^+$	$\gamma p \to (s\bar{s})^* p$
$K^- p \to (K^- K^+) \Lambda$	$K_L p \to (K^+ K^-) \Sigma^+$	
$K^- p \to (K_S K^\pm \pi^\mp) \Lambda$	$K_L p \to (K_S K^\pm \pi^\mp) \Sigma^+$	

A SUMMARY OF THE RESULTS FROM LASS AND THE FUTURE OF STRANGE QUARK SPECTROSCOPY*

D. Aston,[1] N. Awaji,[2] T. Bienz,[1] F. Bird,[1] J. D'Amore,[3]
W. Dunwoodie,[1] R. Endorf,[3] K. Fujii,[2] H. Hayashii,[2] S. Iwata,[2]
W. Johnson,[1] R. Kajikawa,[2] P. Kunz,[1] Y. Kwon,[1] D. Leith,[1] L. Levinson,[1]
J. Martinez,[3] T. Matsui,[2] B. Meadows,[3] A. Miyamoto,[2] M. Nussbaum,[3]
H. Ozaki,[2] C. Pak,[2] B. Ratcliff,[1] P. Rensing,[1] D. Schultz,[1] S. Shapiro,[1]
T. Shimomura,[2] P. Sinervo,[1] A. Sugiyama,[2] S. Suzuki,[2] G. Tarnopolsky,[1]
T. Tauchi,[2] N. Toge,[1] K. Ukai,[4] A. Waite,[1] S. Williams[1]

[1] *Stanford Linear Accelerator Center,*
Stanford University, Stanford, CA 94309, USA
[2] *Nago ya University, Department of Physics,*
Furo-cho, Chikusa-ku, Nagoya-shi 464, Japan
[3] *University of Cincinnati, Department of Physics,*
Cincinnati, OH 45221, USA
[4] *University of Tokyo, Institute for Nuclear Study,*
3-2-l Midori-cho, Tanashi-shi, Tokyo 188, Japan

ABSTRACT

A brief summary is presented of results pertinent to strange quark spectroscopy derived from high statistics data on *K-p* interactions obtained with the LASS spectrometer at SLAC. The present status of strange meson spectroscopy is briefly reviewed, and the impact of the proposed KAON Factory on the future of the subject considered.

Invited talk presented by W. Dunwoodie at the 15th APS Division of Particles and Fields General Meeting, Houston, TX, January 3-6, 1990.

1. INTRODUCTION

This paper summarizes the results on strange quark spectroscopy obtained from an exposure of the Large Aperture Superconducting Solenoid (LASS) spectrometer at SLAC to a K^- beam of 11 GeV/c. The spectrometer and relevant experimental details are described elsewhere.[1,2] The raw data sample contains $\sim$ 113 million triggers, and the resulting useful beam flux corresponds to a sensitivity of 4.1 events/nb. The acceptance is approximately uniform over almost the full 47r solid angle.

2. Ω^{*-} SPECTROSCOPY

Although the Ω^- was discovered in 1962, claims for the observation of Ω^{*-} resonances have been made only recently.[3,4,5] Preliminary evidence for an Ω^{*-} of mass $\sim$ 2.26 GeV/c^2 was reported in the present experiment! Subsequently, evidence for states with masses of 2251 and 2384 MeV/c^2 produced in Ξ^- interactions in beryllium was published!' More recently:' the full data sample from the present experiment has yielded clear evidence for the production of an Ω^{*-} resonance of mass 2253 $\pm$ 13 and width 85 $\pm$ 40 MeV/c^2, thus confirming the preliminary result.[3] The state is observed in the $\Xi^*(1530)\overline{K}$ decaymode, as shown in fig.1a, and the corresponding inclusive cross section is estimated to be 630 $\pm$ 180 nb. It is reasonable to consider this result as confirmation of the 2251 MeV/c^2 state of ref. 4, however there is no evidence for the production of the state of mass 2384 MeV/c^2 in the K^-p data.

The study of inclusive Ω^- production in the present experiment has resulted in the $\Omega^-\pi^+\pi^-$ mass distribution of fig.1b.[6] A clear peak is observed at $\sim$ 2.47 GeV/c^2. Interpreting this as being due to the production of a new Ω^{*-}, the fit denoted by the solid curve yields mass and width estimates of 2474 $\pm$ 12 and 72 $\pm$ 33 MeV/c^2, respectively, and the signal has $\sim$ 5.5σ significance.

In summary, the existence of an Ω^{*-} of mass $\sim$ 2250 MeV/c^2 decaying primarily to $\Xi^*(1530)X$ seems confirmed; moreover, the mass and principal decay mode are quite consistent with theoretical expectations!'" The status of the state at 2384 MeV/c^2 is uncertain, since it is not observed in the present experiment. Finally, the new Ω^{*-} at $\sim$ 2470 MeV/c^2 needs confirmation from other experiments; theoretical predictions concerning possible states in this mass range would also be of interest.

3. K^* SPECTROSCOPY

A principal objective in studying meson spectroscopy is the precise definition of the level structure of the anticipated $q\overline{q}$ meson states. In this regard, the strange sector is particularly favored since it is free, not only from the need for isoscalar-isovector

separation, but also from confusion resulting from the possible production of e.g. $K\overline{K}$ molecule and/or **glueball** states. The quark model level diagram is expected to take the **form**[9] illustrated qualitatively in fig.2 for the **charmonium states.**[10] Here S and L denote total quark spin and orbital angular momentum, respectively, and C indicates the charge conjugation parity of the resulting meson state. The **para-charmonium** levels are singlets, whereas the ortho-charmonium levels, other than ^{3}S, are triplets separated in mass due to spin-orbit interaction. Within each column, the lowest-lying state is the ground state, and the higher states correspond to radial excitations of -this state. By convention, the leading orbital excitations are the ground states with largest total angular momentum, J, and, for the triplet levels, the remaining states are termed the underlying states. In $e^+ e^-$ collisions, the ^{3}S tower of states is readily accessible, while information on the leading orbital excitations with $J \geq 3$ is lacking, and that on the corresponding underlying states is sparse. Results of a complementary nature are obtained from hadronic interaction experiments, where production of the leading orbital states predominates, and precise information on the underlying and radially- excited states requires careful amplitude analyses of high statistics data.

To date the present experiment has provided such information primarily on the natural parity strange meson (i.e.K^*) states. The resulting light quark level structure is related to the nature of the long-range (i.e.confining) part of the $q\overline{q}$ interaction, and thus, in principle, provides information on non-perturbative QCD. In practice, it enables us to learn about QCD potential models incorporating relativistic **corrections.**[11]

The results relevant to K^* spectroscopy in the present experiment are obtained from amplitude analyses of the $\overline{K}^0 \pi^+ \pi^-$ system in the reaction

$$K\text{-}p \rightarrow \overline{K}^0 \pi^+ \pi^- n \tag{1}$$

and of the $K^- \pi^+$, $\overline{K}^0 \pi^-$ and $K^- \eta$ systems produced in the reactions

$$K\text{-}p \rightarrow K^- \pi^+ n \tag{2}$$

$$K^- p \rightarrow \overline{K}^0 \pi^- p \tag{3}$$

and

$$K\text{--}p \rightarrow K^- \eta \, p \; ; \tag{4}$$

these analyses are discussed in detail in refs. 12-15 respectively, and so only the main features will be summarized here.

The analysis of reaction $(1)^{[12]}$ yields the intensity distributions of fig.3 for the natural spin-parity (J^P) states of the $\overline{K}^0 \pi^+ \pi^-$ system. Signals corresponding to

3

the $\overline{K}{}^*_2(1430)$, the $\overline{K}{}^*_3(1780)$ and the $\overline{K}{}^*_4(2060)$ are observed in the 2^+, 3^- and 4^+ distributions, respectively. The 2^+ distribution exhibits a second peak at ~ 2 GeV/c^2, while the 1^- distribution has a shoulder at ~ 1.4 GeV/c^2 followed by a peak at ~ 1.8 GeV/c^2. The $\overline{K}{}^*(892)\pi$ and $\overline{K}\rho(770)$ contributions to the 1^- spectrum are shown in figs.4a,b; the curves result from a description in terms of two Breit-Wigner(BW) resonances. The lower mass state (M=1420$\pm$17, Γ=240$\pm$30 MeV/c^2) approximately decouples from the $K\rho$ channel, and its production characteristics indicate weak coupling to $K\pi$ also; it is most readily interpreted as the first radial -excitation of the $\overline{K}{}^*(892)$. The second state (M=1735$\pm$30, Γ=423$\pm$48 MeV/c^2) may be the underlying member of the ^{3}D ground state; however its mass is greater and its width significantly larger than that obtained from reaction (2)[13] so that it could be a mixture of this state and the second radial excitation of the $K^*(892)$.

A similar fit to the 2^+ data yields mass and width estimates of 1973 $\pm$ 33 and 373 $\pm$ 93 MeV/c^2 respectively for the higher mass state, which corresponds most probably to the first radial excitation of the $\overline{K}{}^*(1430)$,[12] although it may also be a partner to the $K^*_4(2060)$ in the F wave ground state triplet.

The raw $K^-\pi^+$ mass spectrum for reaction (2) is shown in fig.5; the shaded region corresponds to events with M(n π^+)$\geq$ 1.7 GeV/c^2. In addition to an elastic BW amplitude describing the $\overline{K}{}^*(892)$ (cf.fig.9), the amplitude analysis[13] yields the resonant D-H wave signals of fig.6, thereby extending the observed leading orbital states to J^P= 5^-. The corresponding behavior of the underlying S wave amplitude up to 1.6 GeV/c^2 is shown in fig.7. The curves correspond to an effective range parametrization plus a BW amplitude (M=1412 $\pm$ 4 $\pm$ 5, Γ=294 $\pm$10 $\pm$21 MeV/c^2), and the resultant S wave is approximately elastic up to ~ 1.5 GeV/c^2. The state described by the BW is the ^{3}P$_0$ partner of the $\overline{K}{}^*(1430)$. Above 1.8 GeV/c^2, there are two S wave solutions, as shown in fig.8. Both resonate in the 1.9-1.95 GeV/c^2 region, have width ~ 0.2 GeV/c^2 and elasticity ~ 0.5. In the quark model such a state can only be the first radial excitation of the ^{3}P$_0$ ground state.

Finally, the behavior of the P wave $\overline{K}\pi$ scattering amplitude from reaction (2) is shown in fig.9 for the region up to 1.8 GeV/c^2. The solid curve provides a satisfactory description in terms of three BW resonances:[13] (i) the $\overline{K}{}^*(892)$; (ii) a resonance at ~ 1.4 GeV/c^2 of elasticity ~ 0.07 which is consistent with the radial excitation of the $\overline{K}{}^*(892)$ observed in reaction (1); and (iii) a resonance (M=1677 $\pm$10 $\pm$32, Γ=205 $\pm$16 $\pm$34 MeV/c^2) of elasticity ~ 0.39 which is readily interpreted as the ^{3}D$_1$ ground state.

The production mechanism for reactions (1) and (2) is predominantly unnatural parity, helicity zero exchange. In contrast, the $\overline{K}{}^0\pi^-$ system in reaction (3)[14] is produced mainly by natural parity, helicity one exchange (cf. fig.10). Nevertheless, a description of the mass dependence of the resulting amplitudes and relative phases

4

requires the same P, D and F wave resonance structure found for reactions (1) and (2). This is illustrated in fig.11, where the solid curves correspond to three P wave resonances, two D wave resonances, and one F wave resonance. Clearly, these structures are required in order to reproduce the relative phase motion, and the parameter values obtained from reaction (3) agree well with those obtained from reactions (1) and (2).

In general, theoretical predictions"" are in quite good agreement with these measurements. However, the $^3P_0$ ground state is predicted $\sim$ 170 MeV/c^2 low, and the $^3S_1$ first radial excitation is predicted $\sim$ 160 MeV/c^2 high with respect to the measure&mass value. Also, for the $^3S_1$ and $^3P_0$ levels the expected splitting between the ground state and first radial excitation is $\sim$650-680 MeV/c^2, whereas it is observed to be $\sim$500-550 MeV/c^2. It should be noted also that for the $^3S_1$ states this splitting is predicted to increase from the charmonium to strange meson sector; it appears actually to decrease by -70 MeV/c^2.

Reaction (4) has been measured with large statistics for the first time in the present experiment, and the resulting $K^-\eta$ mass spectrum is shown in fig.12. An amplitude analysis of the $K^-\eta$ system[15] has established that the peak at -1.8 GeV/c^2 results from production of the $\overline{K}^*_3(1780)$ (cf.fig.13). This, together with the results of a similar analysis of reaction (3),[14] yields a branching fraction to $\overline{K}\eta$ of 7.7±1.0%, in accord with SU(3). SU(3) predicts also that K^* states of even spin couple only weakly to $K\eta$. This is confirmed by the D wave intensity distribution of fig.13. No $\overline{K}^*_2(1430)$ signa is observed, and a 95% confidence level upper limit on the branching fraction is established at 0.45%. This value is an order of magnitude smaller than that obtained from previous low statistics measurements.

4. $s\overline{s}$ SPECTROSCOPY

The processes most relevant to the study of $s\overline{s}$ (i.e.strangeonium) spectroscopy are those in which a $K\overline{K}$ or $K\overline{K}\pi$ system is produced against a recoil hyperon. The objectives in studying such processes are basically the same as for the strange sector. However, in recent years candidate glueball states which also couple to these meson systems have emerged from the study of J/ψ decay. Consequently, it has become increasingly important to define the $s\overline{s}$ level structure in order to distinguish those states which may be of a different dynamical origin. In the present experiment, the relevant reactions which have been studied are

$$K^-p \rightarrow K^0_S K^0_S \Lambda_{seen} \tag{5}$$

$$K^-p \rightarrow K^-K^+ \Lambda_{seen} \tag{6}$$

5

and

$$K\text{-}p \rightarrow K_S^0 K^{\pm} \pi^{\mp} \Lambda_{seen} . \tag{7}$$

They are characterized by peripheral (i.e.quark exchange) production of the meson system, and it follows that the creation of **glueball** states should be disfavored in such processes. Although the data samples are considerably smaller than for reactions (1)-(4), amplitude analyses have been performed,[2,16,17,18] the results of which are summarized here.

The raw $K\overline{K}$ mass distributions for reactions (5) and (6) (fig.14) differ, since for the-former only even spin states are produced. In addition, for reaction (6), the mass region above -1.7 GeV/c^2 is dominated by the reflection of diffractive production of low mass ΛK^+ systems.[19] In fig.15, the $K_S^0 K_S^0$ mass spectrum from reaction (5) is compared to the MARK III data on radiative J/ψ decay[20] in the mass region below 1.9 GeV/c^2 (the LASS data have been scaled to the MARK III data at the peak of the $f_2'(1525)$). Both spectra show a small, but intriguing, threshold rise,[2,21] followed by activity in the $f_2(1270)/a_2(1320)$ region and then the large $f_2'(1525)$ peak. At higher mass, the MARK III spectrum is dominated by the $f_2(1720)$. There is no evidence for any such signal in the LASS distribution, and the upper limit on the production cross section is 94 nb. at the 95% confidence level; it should be noted also that there is no evidence for $f_2(1720)$ production in reaction (7) in the present experiment[16] (cf.fig.21f). These results indicate that the $f_2(1720)$ is indeed a strong candidate **glueball** state.

The amplitude analysis of reaction (5)[2] yields the S wave intensity distribution of fig.16a. Although the uncertainties are large, the data seem to peak in the range $\sim$ 1.5-1.6 GeV/c^2. A similar distribution (fig.16b) has been obtained in an analysis of reaction (6) at 8.25 GeV/c,[22] and there are indications of S wave structure at this mass from the data on reaction (6) in the present experiment. These results suggest the existence of a 0^+ state in this mass region which is naturally interpreted as a partner of the $f_2'(1525)$ in the ^3P ground state. It is not clear whether this state might be identified with the $f_0(1590)$,[23] although the latter appears not to couple strongly to $K\overline{K}$. An immediate consequence of this observation is that the $f_0(975)$, which is usually assigned to this multiplet, may well be a weakly bound $K\overline{K}$ system,[24] or be of some other non-$q\overline{q}$ origin. This is discussed at greater length in ref.2.

For the $K\overline{K}$ system in reaction (6), the acceptance corrected spherical harmonic moments ($t_L^M = \sqrt{4\pi}N\langle Y_{LM}\rangle$; $L \leq 8$, M=O) in the t-channel **helicity** frame are shown in fig.17 for the mass region 1.68-2.44 GeV/c^2, and $t' \leq 0.2$ (GeV/c)^2. It should be noted that amplitudes with spin J can contribute to moments with L$\leq$2J. There is a peak in the mass spectrum, t_0^0, at $\sim$ 1.86 GeV/c^2, and similar structure is present for all moments with L $\leq$ 6, but is absent for L $\geq$ 7. This, together with the absence of such a signal for reaction (5),[2] indicates the presence of a $J^{PC}= 3^{--}$, mostly $s\overline{s}$ state.

6

A detailed analysis of this **region**[17] yields the total F wave intensity distribution of fig.18a for $t' \leq 1.0(\mathrm{GeV/c})^2$; the fitted curve gives BW mass and width 1855 $\pm$ 22 and 74 $\pm$ 67 MeV/c^2, respectively. A similar fit to the mass spectrum (fig.18b) gives parameter values 1851 $\pm$ 9 and 66 $\pm$ 29 MeV/c^2, in agreement with previous measurements from the mass distribution only.[25,26] It should be noted that the spin of this state, which is listed as the $\phi_J(1850)$,[10] is established by the LASS data, and that the mass and width have been estimated for the first time on the basis of an amplitude analysis.

A significant $J^P = 3^-$ signal (fig.21g) has been obtained in the $\phi_3(1850)$ region from the partial wave analysis of reaction (7).[16] This signal, after all corrections, is shown in fig.18c (open dots) in comparison with that from reaction (6) (solid dots); the branching ratio obtained is $BR[(\phi_3(1850) \rightarrow (K^*\overline{K} + c.c.))/(\phi_3(1850) \rightarrow K\overline{K})]$ = $0.55^{+0.85}_{-0.45}$, in agreement with theory!

The $\phi_3(1850)$ is interpreted as belonging to the $^3D_3$ quark model **nonet** which also includes the $\rho_3(1690)$, the $\omega_3(1670)$, and the $K_3^*(1780)$. Using current mass **values**,[10] the mass **formula**[27] yields an octet-singlet mixing angle of $\sim 30°$. This indicates that the multiplet is almost ideally mixed, and that the $\phi_3(1850)$ is an almost pure $s\overline{s}$ state, in accord with its production characteristics.

The analysis of the ϕ_3 **region**[17] has shown-that the peaks observed in fig.17 are due to interference between the resonant F wave and the approximately imaginary amplitude describing the diffractive production of the low mass ΛK^+ system. In fig.17, there is also a small signal in every moment with L ≥ 1 at ~ 2.2 GeV/c^2; no such signal is observed for L ≥ 9. This indicates the existence at this mass of a small, resonant 4^+ amplitude which interferes with the large, imaginary, diffractive background, just as for the ϕ_3. An analysis based on this **interpretation**[18] yields mass and width values of 2209 $^{+17}_{-15}$ and 60 $^{+107}_{-57}$ MeV/c^2 for this $J^{PC} = 4^{++}$ state. These values are consistent with those obtained by MARK III for the X(2220),[20] and with a signal in the $\eta\eta'$ mass spectrum observed by the GAMS collaboration.[28] In addition, the $K\overline{K}$ mass distribution from reaction (5) in this region has been **shown**[2] to be very similar to that observed for radiative J/ψ decay (fig.19). This suggests that the X(2220), which has been conjectured to be a **glueball** state, may instead be a member of the quark model $^3F_4$ ground state **nonet**.

The raw $K\overline{K}\pi$ mass spectrum for reactions (7) (fig.20) exhibits a small signal at the $f_1(1285)$, followed by a rapid rise at $K\overline{K}^*$ threshold to a peak at ~ 1.5 GeV/c^2, and a second peak at ~ 1.9 GeV/c^2. The low mass structure is similar to that observed at 4.2 GeV/c.[29] An amplitude **analysis**[16] yields the partial wave intensity distributions of fig.21. The low mass peak is associated primarily with 1^+ waves, while the 1.9 GeV/c^2 bump is due mainly to 2^- and the 3^- contribution discussed previously. Only K^* or $\overline{K}^*$ isobar production is important; amplitudes involving the $a_0(980)$ are

negligibly small. The 1^+ intensity at low mass shows a pronounced asymmetry in favor of the $\overline{K^*}$ isobar, and also exhibits $K^*\text{-}\overline{K^*}$ interference, which is destructive near threshold, and constructive at ~ 1.5 GeV/c^2. This suggests the existence of two 1^+ states of opposite G-parity in this region. The corresponding J^{PG} amplitude combinations yield 1^{++} and 1^{+-} production intensity distributions (fig.22) which are well described as BW resonances of mass 1.53 ± 0.01 and 1.38 ± 0.02 GeV/c^2 respectively, with corresponding widths 0.10 ± 0.04 and 0.08 ± 0.03 GeV/c^2. The 1^{++} state confirms an earlier observation,[29] while the 1^{+-} state is new. If these are isoscalars,[29] the lower mass state, the $h_1(1380)$, completes the $J^{PC}=1^{+-}$ ground state nonet, while the higher mass state, the $f_1(1530)$, is a strong candidate to replace the $E/f_1(1420)$ in the corresponding 1^{++} nonet. Use of the $f_1(1530)$ in this nonet gives a mixing angle $\sim 55°$; this implies that the $f_1(1530)$ is mainly $s\,\overline{s}$ and that the $f_1(1285)$ has little $s\,\overline{s}$ content, in agreement with their production characteristics. This is not the case when the E is used, since its production properties are not consistent with the predicted large $s\,\overline{s}$ content. Finally, a previous analysis[30] of the 1^{++} nonet made use of the E mass and width to predict an a_1 mass of ~ 1.47 GeV/c^2; when the $f_1(1530)$ mass and width are used instead, the predicted mass is ~ 1.28 GeV/c^2, in much better agreement with the accepted value.[10]

The 1^+ states observed in the present experiment satisfactorily complete the ground state $^1P_1$ and $^3P_1$ quark model nonets. Furthermore, the small spin-orbit interaction implied when the new information on the 0^+ is also taken into account contrasts markedly with the corresponding behavior in the charmonium sector. The status of the E meson as a $q\,\overline{q}$ state is dubious. However, it may be that its proximity to $K\overline{K^*}$ threshold is significant in that it could be a $K\overline{K^*}$ molecule or four-quark state of some kind.

5. STATUS OF THE SPECTROSCOPY

A somewhat optimistic summary of the observed $q\,\overline{q}$ levels in the strange meson sector is presented in fig.23. This includes results from the present experiment, together with information derived from analyses of the charged $K\pi\pi$, $K\phi$ and $\Lambda\overline{p}/\overline{\Lambda}p$ systems.[10] Of the unnatural parity levels with J^P other than 0^-, only the $J^P = 1^+$ ground state has been resolved into the states corresponding to different quark total spin; consequently, the remaining such entries in the left and right halves of fig.23 are identical. The second radial excitation in the 0^- tower is shown as a dashed line since, of the two experiments analyzing $K\phi$,[31,32] only one finds a significant 0^- amplitude.[31]

Some comments regarding the level splittings compared to those predicted have been made already in section 3. In a more empirical vein, the level structure appears

to depend in first approximation only on principal quantum number value; i.e. there is approximate mass degeneracy of states having different spin-parity but the same value of the (orbital+radial) excitation quantum numbers. A notable exception involves the S wave ground states; this suggests that the spin-spin interaction is large only in this configuration.

For the triplet states, the spin-orbit interaction, as measured by the mass difference between the leading state and the other natural parity member of the triplet, appears to increase approximately linearly as (J-l), where J is the spin of the leading state, This might be expected from simple angular momentum considerations. However, the behavior of the unnatural parity triplet member does not conform to such a pattern at all. For the ground state triplets, the unnatural parity state relative to the leading state is ~ 100 MeV/c^2 low for the P wave, about equal for the D wave, and ~ 250 MeV/c^2 high for the F wave, if the reported 3^+ state is the ground state. This in fact, may not be the case, since for the G wave the difference is only ~ 100 MeV/c^2; however the behavior is still anomalous. In addition, for the first radially excited P wave triplet, the unnatural parity state appears to be at least twice as far below the leading state as it is in the ground state triplet. It would appear difficult to reproduce such behavior in a simple potential model, and so it would be of interest to attempt to fit the structure observed in fig.23 by means of models such as that of reference 11.

A similar summary is presented in fig.24 for the mainly $s\bar{s}$ sector. Information on radial excitations is sparse, and in this regard the 0^- states observed by Mark III in $\phi\phi$ and $K^*\overline{K^*}$[33,34] and the 2^+ states observed in hadronic $\phi\phi$ production[35] have been somewhat arbitrarily included; it is difficult to assess the extent to which they might really belong in such a picture. The spin-spin interaction in the S wave ground state again appears to be large. Furthermore, the limited information available on the ground state triplets indicates that the spin-orbit interaction is rather weak and does not exhibit the anomalous behavior observed for the strange sector. Clearly, much experimental work needs to be done in order to bring the information on the $s\bar{s}$ sector even to the level of that on the strange sector.

6. THE FUTURE: KAON

The LASS experiment has demonstrated:

(i) the effectiveness of a programmatic approach to the study of meson spectroscopy;

(ii) the feasibility of obtaining very large statistics in a fixed target experiment by running a 4π acceptance spectrometer in interaction mode;

(iii) that the corresponding computing requirements can be met by means of a combination of large mainframe and microprocessor farm availability;

(iv) that the resultant large data samples for individual reactions can be analyzed in a relatively straightforward manner;

(v) the value of being able to analyze many different channels in the same experiment under conditions of uniform and well-understood acceptance;

(vi) that such a program need not involve a large number of physicists and graduate students.

In the next ten years, it would be desirable to push such a program to a significantly higher statistical level, while maintaining the uniform acceptance which characterizes the LASS experiment. This would imply an experiment of something like five billion triggers. Such experiments are already contemplated at Fermilab, (e.g. E791) and it seems that the data processing, storage and retrieval needs can be met. The level structure of fig. 23 would be significantly refined by such a program, and that of fig.24 would be carried beyond the present-day understanding of the strange sector. In addition, a programmatic study using pion beams should be carried out in order to similarly advance the understanding of the isovector and non-$s\bar{s}$ sectors.

The first requirement for the successful implementation of such a program is that it should form a significant component of the overall program of the lab. in which it is situated; significant long-term commitment of lab. resources is involved. There should be strong in-house involvement in the experiments for purposes of continuity and support, but there should also be an active and enthusiastic external user group. Constructive in-house theoretical interest would also be desirable. The facilities should include a high-intensity r.f. separated beam in order that data can be acquired in six months to a year of running. The spectrometer should be an upgraded LASS-type detector; it should have better resolution, photon detection, silicon vertex detector, etc., and should be able to cope with data transfer rates of at least five megabytes/sec. There should be powerful mainframe computing on-site together with a sizable microprocessor farm and extensive data storage and retrieval capability; a network of user-friendly low-end work-stations should also exist.

The most likely place for most of these ingredients to come into being on the indicated time-scale is at TRIUMF by means of the KAON Factory project. The present plans call for an r.f. separated beam line in the 6-20 GeV/c range providing $\sim 10^7$ K's per spill. They are favoring a spectrometer facility which is something of a cross between LASS and the Crystal Barrel detector at LEAR. Furthermore, this spectrometer facility figures prominently in the planned program of the lab., thereby indicating strong in-house commitment. There appears to be enthusiasm for such a facility among the user community, and development of the computing capabilities of the lab. along the lines indicated above is being considered.

It seems clear that the future of strange quark spectroscopy in particular, and indeed of light quark spectroscopy in general, is tied to the existence of the KAON Factory. The programmatic approach to the study of meson spectroscopy over the last twenty years or so at SLAC has proven its worth. However, there is much that remains to be understood, and it would seem that this greater understanding can only be achieved by means of the higher level, long-term program embodied in KAON.

7. CONCLUSION

The present experiment has made significant contributions to the various areas of strange quark spectroscopy discussed above. Data analysis is continuing, and new results will be forthcoming on inclusive Ξ^- and Ξ^* production, the $K^-\omega p$ final state, and the production of meson systems such as K^*K^*, $\phi\phi$, $\phi\pi$, and $\pi^+\pi^-$ against a recoil A. Indeed, preliminary results from some of the hypercharge exchange reactions have already been presented?'

Future advances in the area of light quark spectroscopy require the kind of programmatic approach which has been adopted at SLAC over the last twenty years or so, but at a significantly higher statistical level and including experiments of a similar nature with incident pions. It is probable that such broad advances can be made only by means of an upgraded LASS-type detector located at the KAON Factory, and consequently that the future of the subject is intimately bound to the approval and construction of this facility.

REFERENCES

1. D. Aston et al., The LASS Spectrometer, SLAC-REP-298 (1986).

2. D. Aston et al., Nucl. Phys. B301, 525 (1988).

3. D. Aston et al., contributed talk given by B. Ratcliff in session PO9 at the International Europhysics Conference on High Energy Physics, Bari, Italy, July 1985; see S. Cooper, Rapporteur Talk in the Proceedings of this Conference, p. 947 and SLAC-PUB-3819.

4. S.F. Biagi et al., Z. Phys. C31, 33 (1986).

5. D. Aston et al., Phys. Lett. 194B, 579 (1987).

6. D. Aston et al., Phys. Lett. 215B, 799 (1988).

7. N. Isgur and G. Karl, Phys. Rev. D19, 2653 (1979).

8. K.T. Chao, N. Isgur and G. Karl, Phys. Rev. D23, 155 (1981).

9. W. Grotrian, Graphische Darstellung der Spektren von Atomen und Ionen mit ein, zwei und drei Valenzelektronen (Springer, Berlin, 1928).

10. Particle Data Group, Phys. Lett. 204B (1988).

11. S. Godfrey and N. Isgur, Phys. Rev. D32, 189 (1985).

12. D. Aston et al., Nucl. Phys. B292, 693 (1987).

13. D. Aston et al., Phys. Lett. 180B, 308 (1986); Nucl. Phys. B296, 493 (1988).

14. P.F. Bird, Ph.D. Thesis, SLAC Report 332 (1988).

15. D. Aston et al., Phys. Lett. 201B, 169 (1988).

16. D. Aston et al., Phys. Lett. 201B, 573 (1988).

17.-D. Aston et al., Phys. Lett. 208B, 324 (1988).

18. D. Aston et al., Phys. Lett. 215B, 199 (1988).

19. D. Aston et al., SLAC-PUB-4202 / DPNU-87-08 (1987).

20. R.M. Baltrusaitis et al., Phys. Rev. Lett. 56, 107 (1986).

21. K.L. Au et al., Phys. Rev. D35, 1633 (1987).

22. M. Baubillier et al., Z. Phys. C17, 309 (1983).

23. D. Alde et al., Phys. Lett. 201B, 160 (1988), and references therein.

24. J. Weinstein and N. Isgur, Phys. Rev. Lett. 48, 659 (1982); Phys. Rev. D27, 588 (1983), and references therein.

25. S. Al-Harran et al., Phys. Lett. 101B, 357 (1981).

26. T. Armstrong et al., Phys. Lett. 110B, 77 (1982).

27. M. Gell-Mann, Caltech report TSL-20 (1961) unpublished;
    S. Okubo, Prog. Theor. Phys. (Kyoto) 27, 949 (1967).

28. D. Alde et al., Phys. Lett. 177B, 120 (1986).

29. Ph. Gavillet et al., Z. Phys. C16, 119 (1982).

30. R.K. Carnegie et al., Phys. Lett. 68B, 287 (1977).

31. T. Armstrong et al., Nucl. Phys. B221, 1 (1983).

32. D. Frame et al., Nucl. Phys. B276, 667 (1986).

33. G. Eigen, CALT-68-1595 (1989).

34. Z. Bai et al., SLAC-PUB-5159 (1990).

35. A. Etkin et al., Phys. Lett. 201B, 568 (1988).

36. D. Aston et al., SLAC-PUB-5150 (1989).
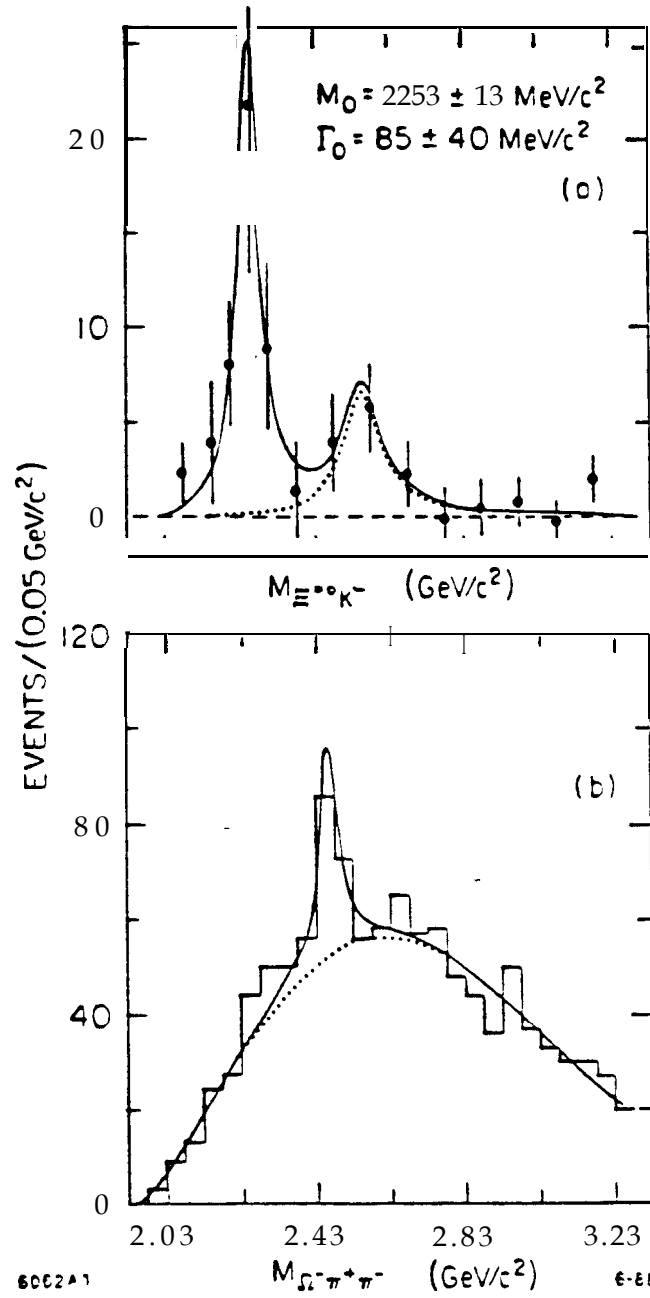
Fig.1.(a) The inclusive $\Xi^{*0}(1530)K^-$ mass distribution; the solid curve is the result of a fit using two Breit-Wigner line-shapes. (b) The inclusive $\Omega^-\pi^+\pi^-$ mass distribution; the solid curve is the result of a fit using a Breit-Wigner line-shape and a polynomial background.

13

(c̄c LEVEL SCHEME)

	S = 0				S = 1			
L	0	1	2	3	0	1	2	3
s	+	−	+	−	−	+	−	+

					ψ (4415)			
					ψ (4160)	− − − − − − − − −	− − − − − − − − −	− − −4⁺ − − −3⁺ − − −2⁺
	− − −	− − −	− − −	− − − 3⁺⁻	ψ (4030)	− − − − − − − − −	− − −3⁻ − − −2⁻ 1⁻	
	− − −	− − −	− − − 2⁻⁺		ψ (3685)		ψ (3770)	
	− − −	− − − − 1⁺⁻			⫫	2⁺ 1⁺ 0⁺	χ₂(3555) χ₁(3510) χ₀(3415)	
					J/ψ (3097) 1⁻⁻			
	η_c(2980) 0⁻⁺							

| 1-87
5646A9 | ¹S | ¹P | ¹D | ¹F | ³S | ³P | ³D | ³F |

Fig.2. The quark model level diagram for the charmonium states; the mass scale is only qualitative.

14
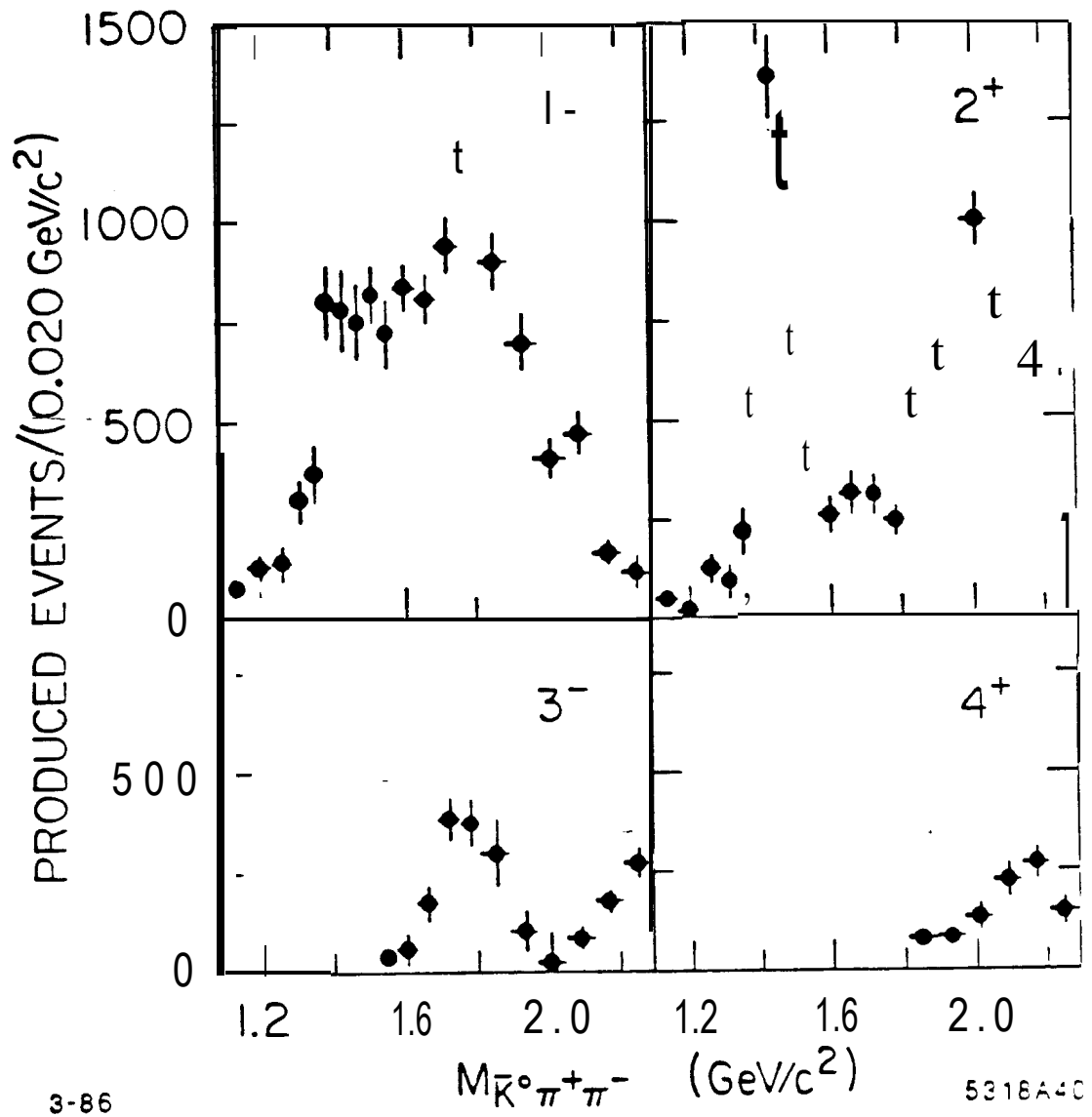
Fig.3. The natural spin-parity intensity distributions obtained from the amplitude analysis of reaction (1).
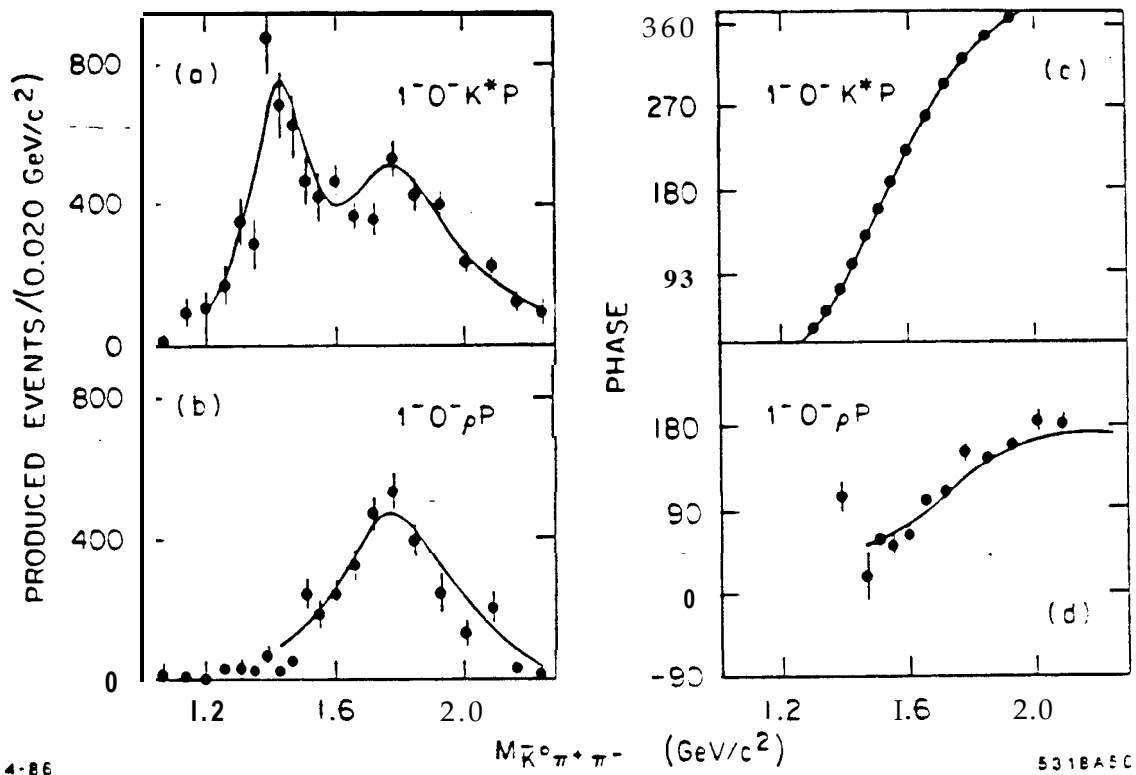
Fig.4. The individual isobar contributions to the 1^- distribution of fig.3; the curves are described in ref. 12.

16
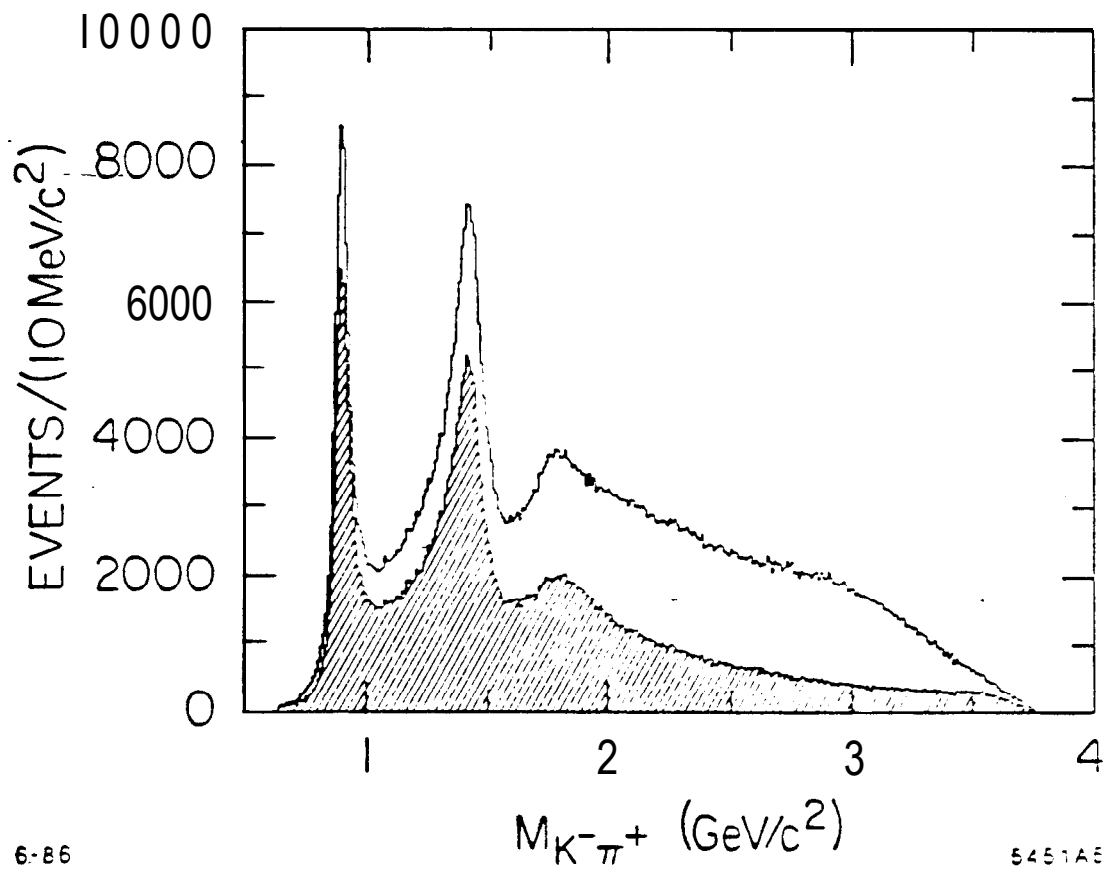
Fig.5. The raw $K^-\pi^+$ mass distribution for reaction (2); the shaded region corresponds to events with $M(n\ \pi^+) \geq 1.7$ GeV/c^2.

17
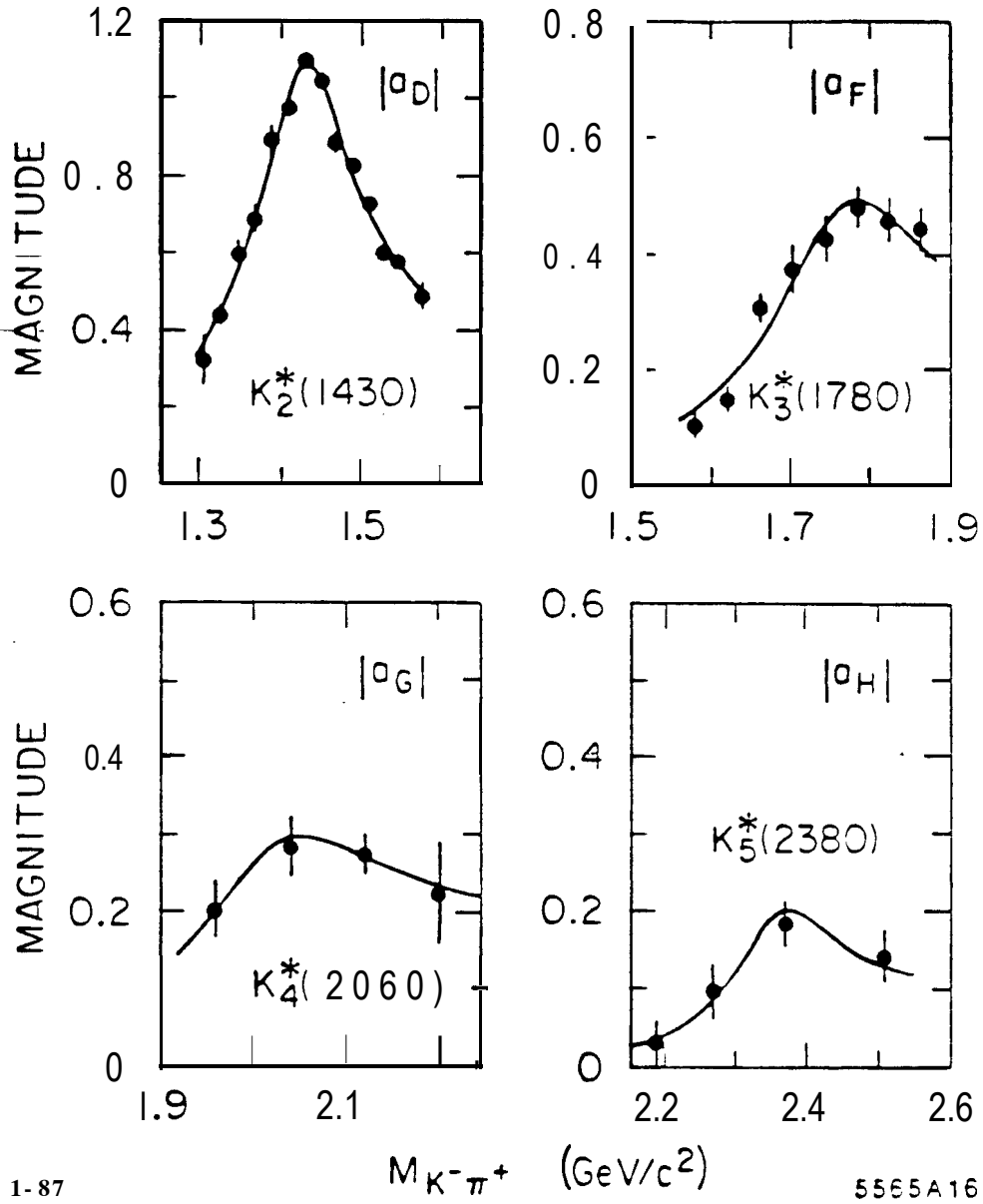
Fig.6. The mass dependence of the amplitudes of the leading orbital states obtained from reaction (2).
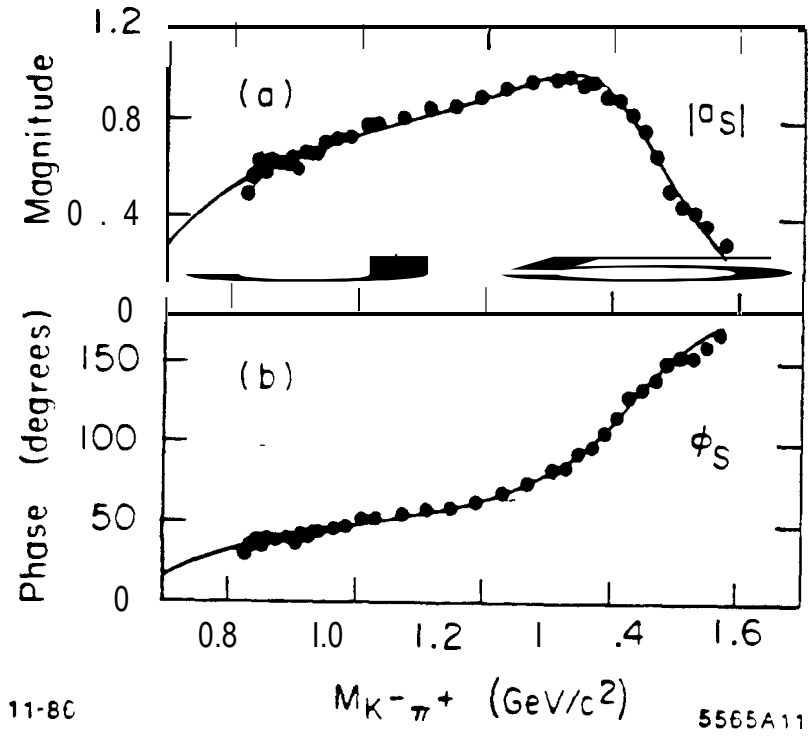
Fig.7. The behavior of the S wave $\overline{K}\pi$ scattering amplitude up to 1.6 GeV/c^2 from reaction (2); the curves are described in ref.13.

19
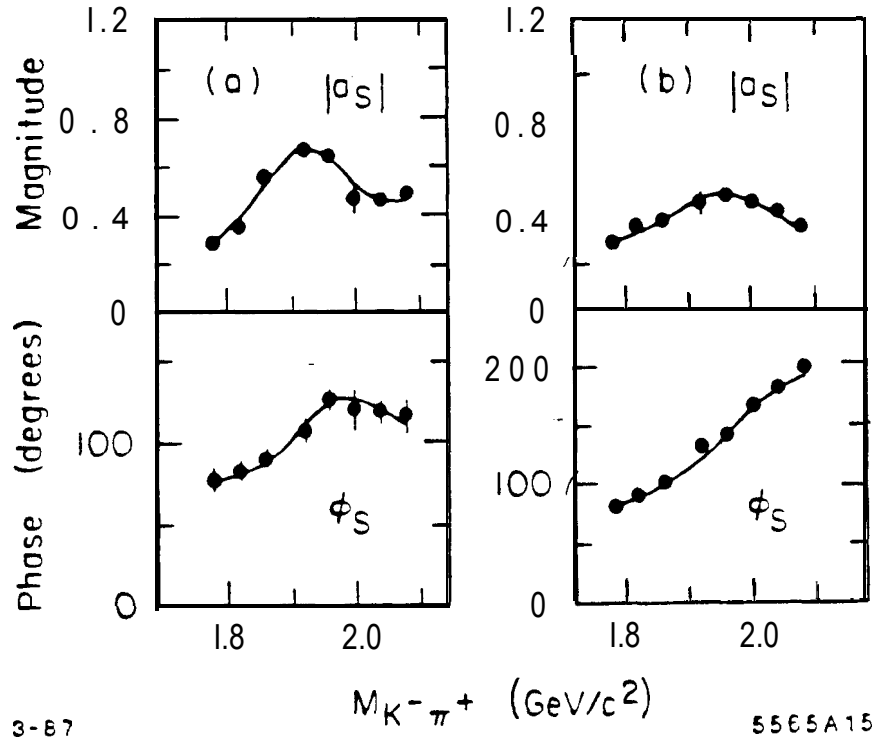
Fig.8. The behavior of the S wave $\overline{K}\pi$ scattering amplitude solutions above 1.8 GeV/c^2 from reaction (2); the curves are described in ref.13.

20
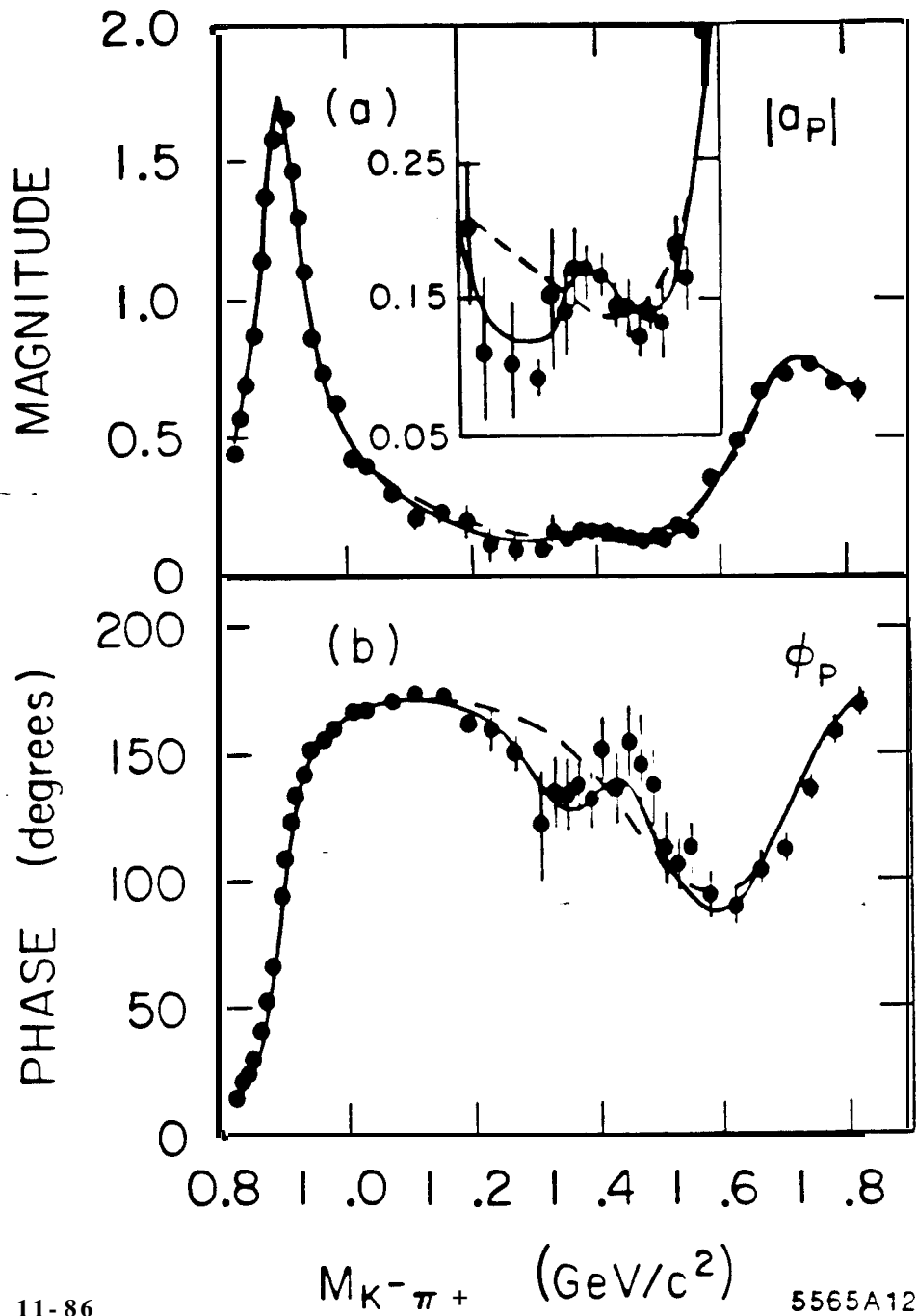
Fig.9. The behavior of the P wave $\overline{K}\pi$ scattering amplitude up to 1.8 GeV/c^2 from reaction (2); the curves are described in ref.13.
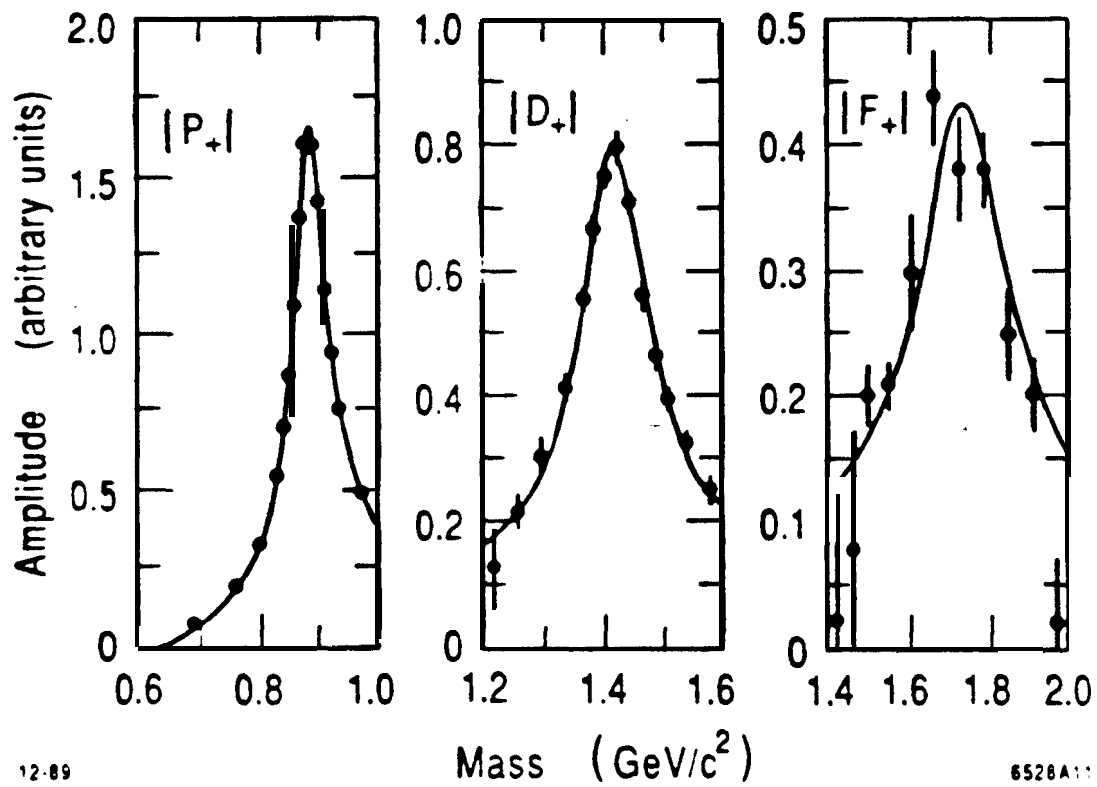
Fig.10. The mass dependence of the leading $\overline{K^*}$ amplitudes from reaction (3); the subscript indicates that production is via helicity one natural parity exchange in the t channel.

22
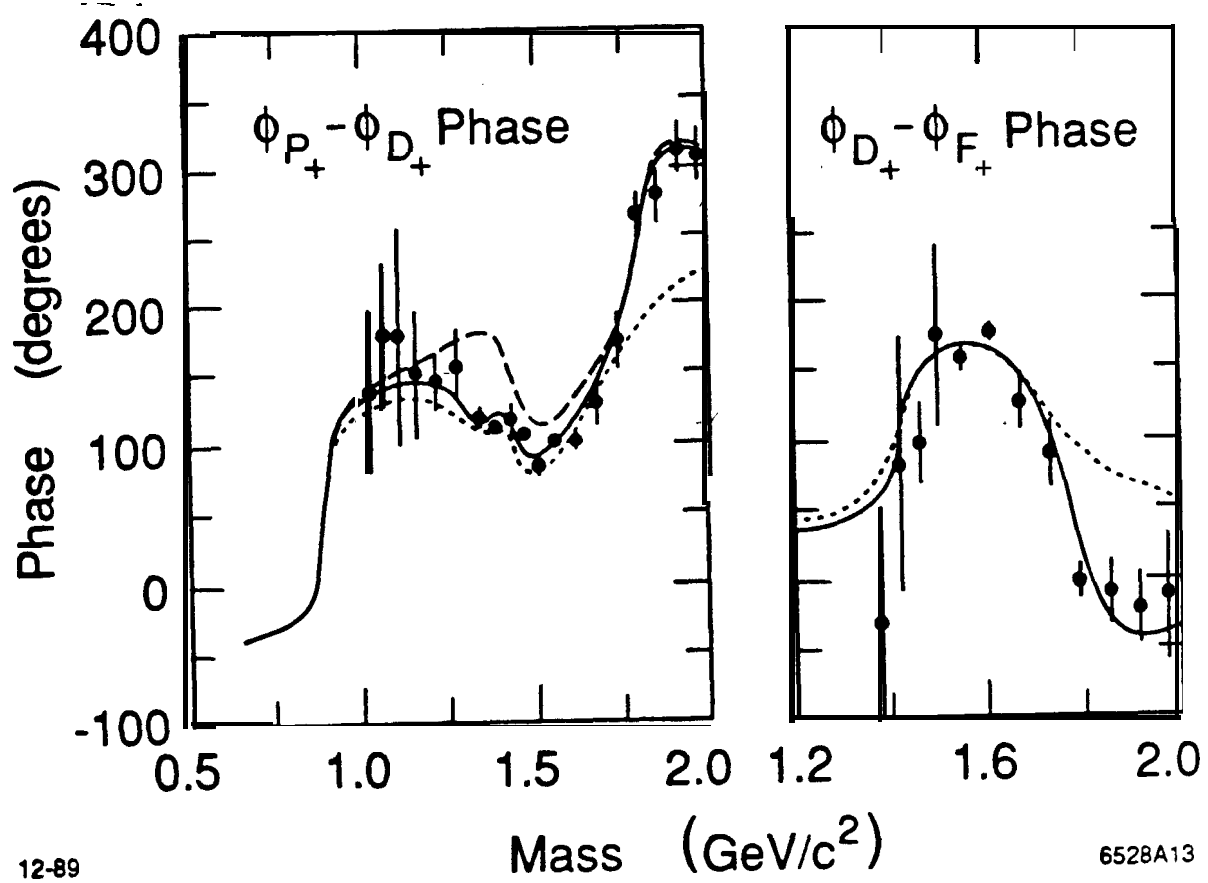
Fig.11. The mass dependence of the relative phase between the P-D and D-F amplitudes of fig.10; the solid curves are described in the text; the dotted curve is obtained if the second D wave resonance is excluded; the dashed curve is obtained if the small P wave resonance at ~ 1.4 GeV/c^2 is excluded.
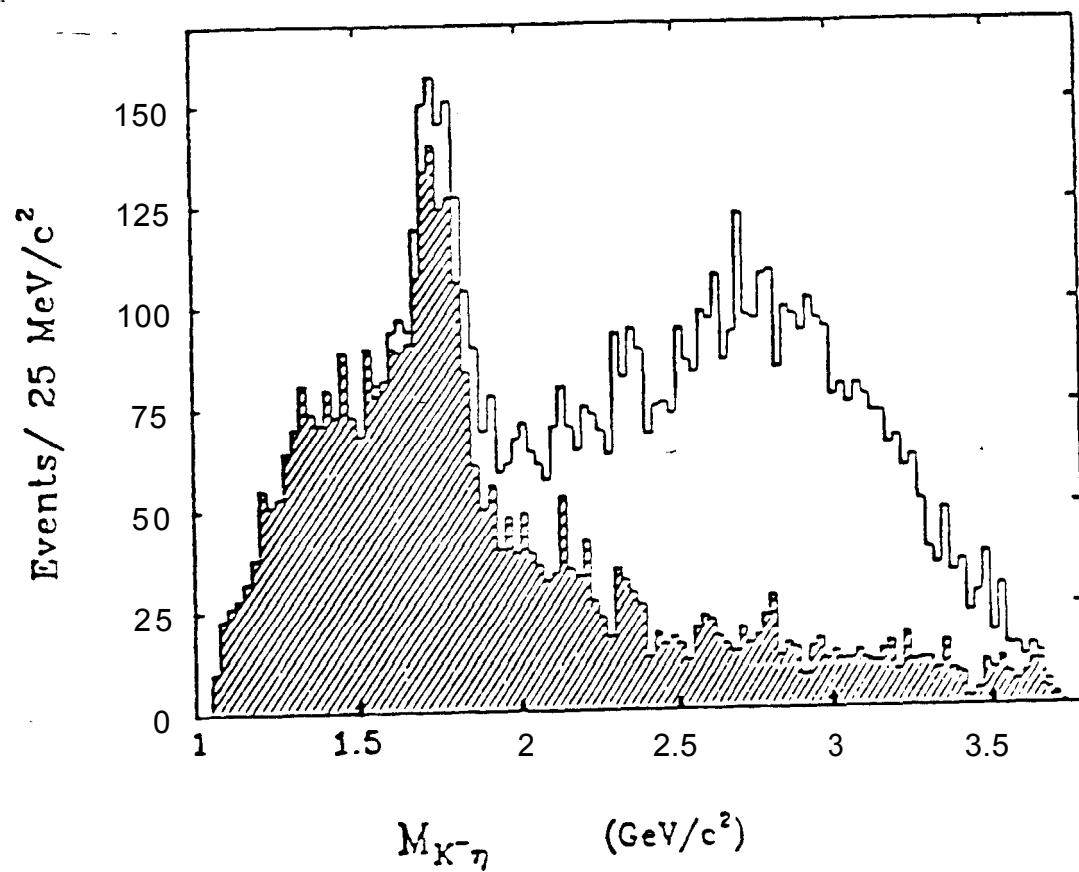
Fig.12. The $K^-\eta$ mass distribution from reaction (4); the shaded region corresponds to $M(\eta p) \geq 2.0$ GeV/c^2 and $M(K^- p) \geq 1.85$ GeV/c^2.

24
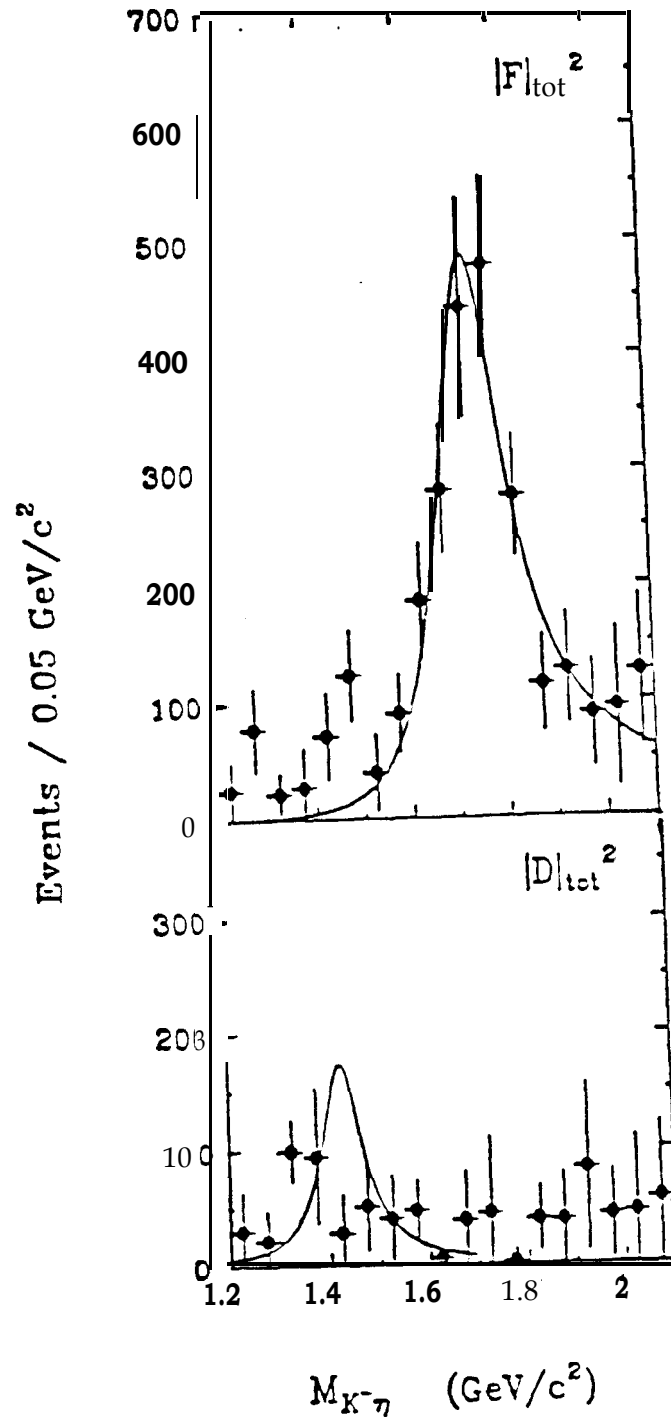
Fig.13. The total F and D wave intensity distributions from reaction (4); the F wave curve corresponds to a $\overline{K}^*_3$ (1780) BW; the D wave curve indicates the 95% confidence level limit on $\overline{K}^*_2$ (1430) production.

25
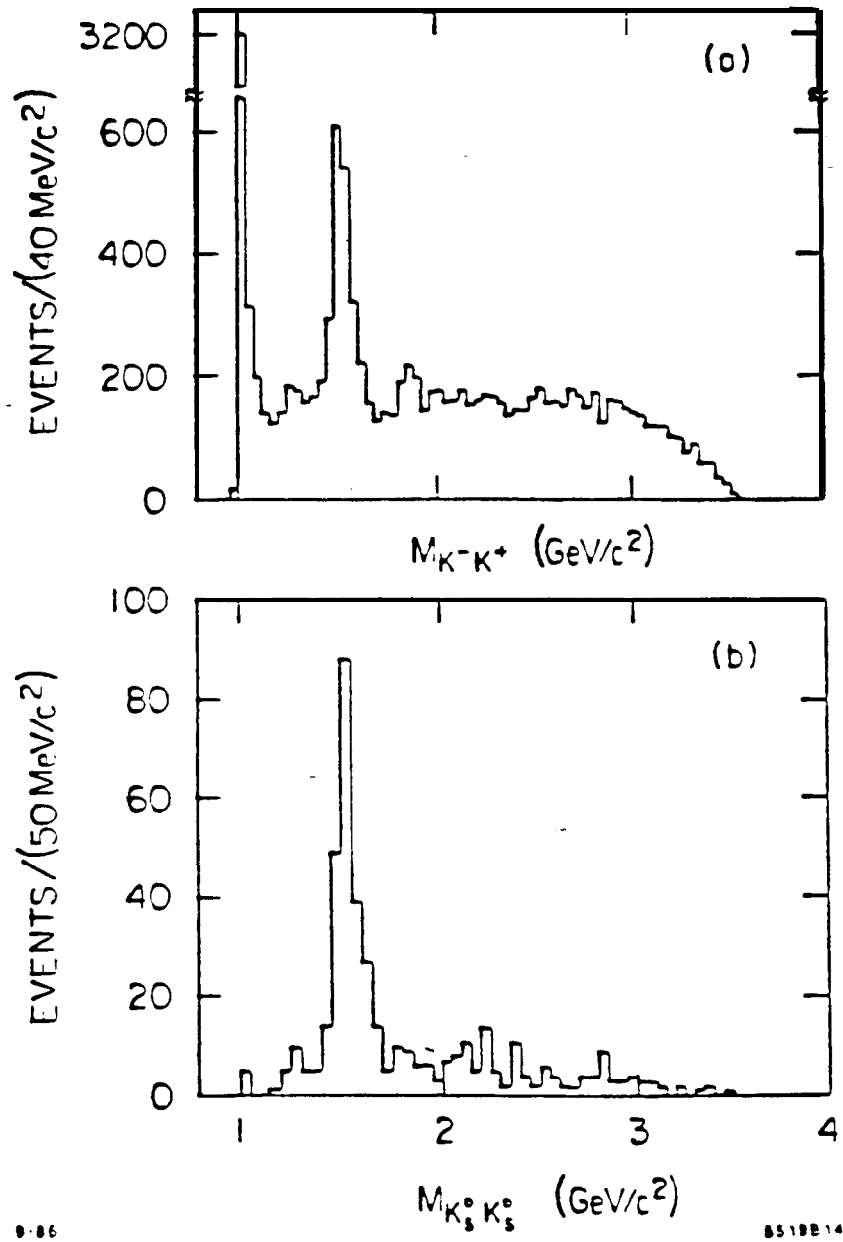
Fig.14. The $K\overline{K}$ mass projections for reactions (5) and (6).
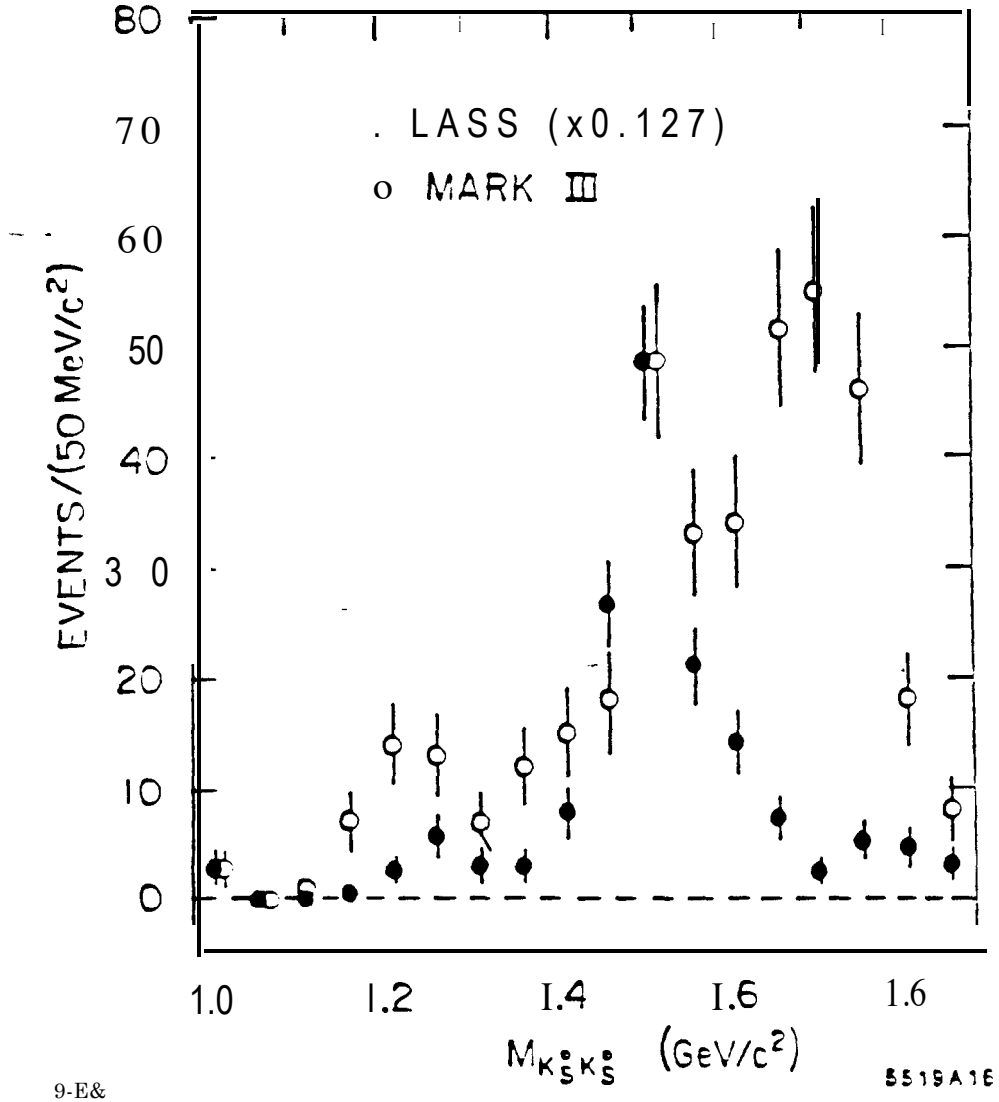
Fig.15. The comparison of the $K_S^0 K_S^0$ mass distribution from reaction (5) with that from radiative J/ψ decay[20] from threshold up to 1.9 GeV/c^2.

27
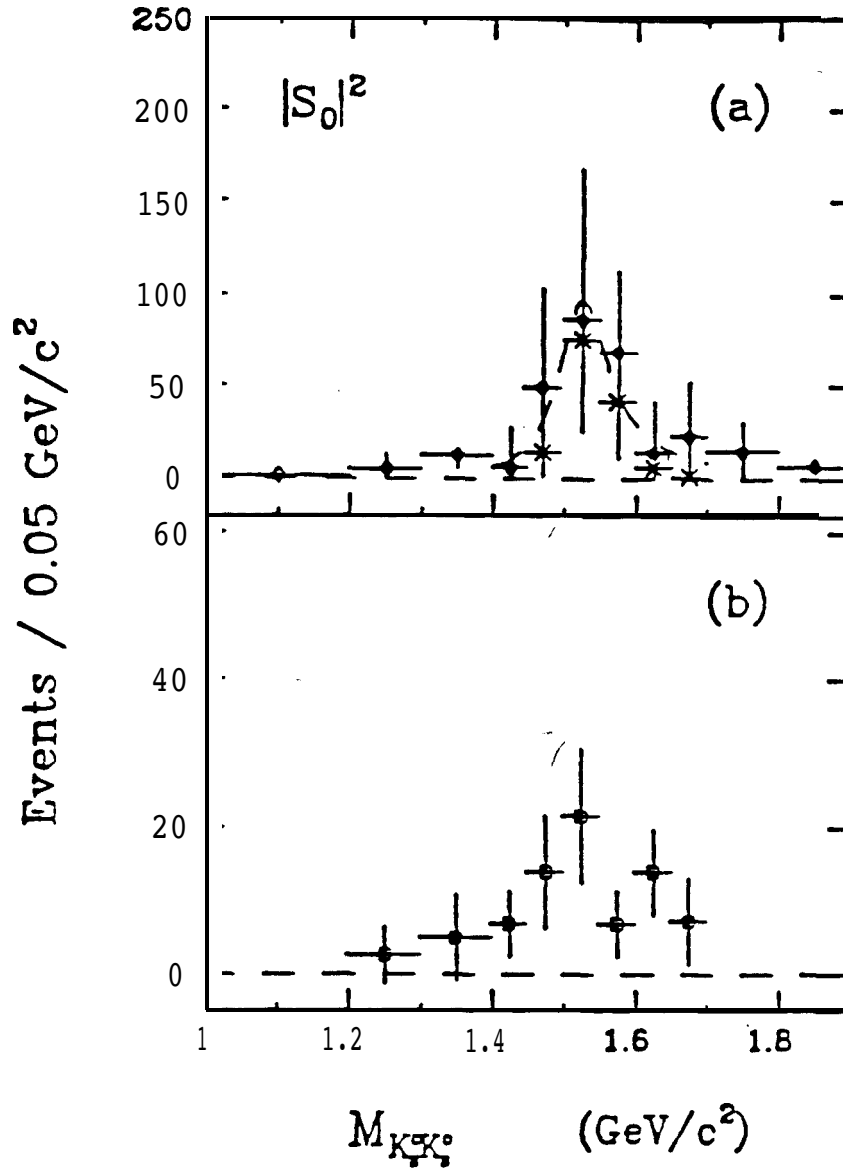
Fig.16. (a) The S wave intensity distribution from the amplitude analysis of reaction (5). (b) The S wave intensity distribution from the amplitude analysis of reaction (6) at 8.25 GeV/c.[22]
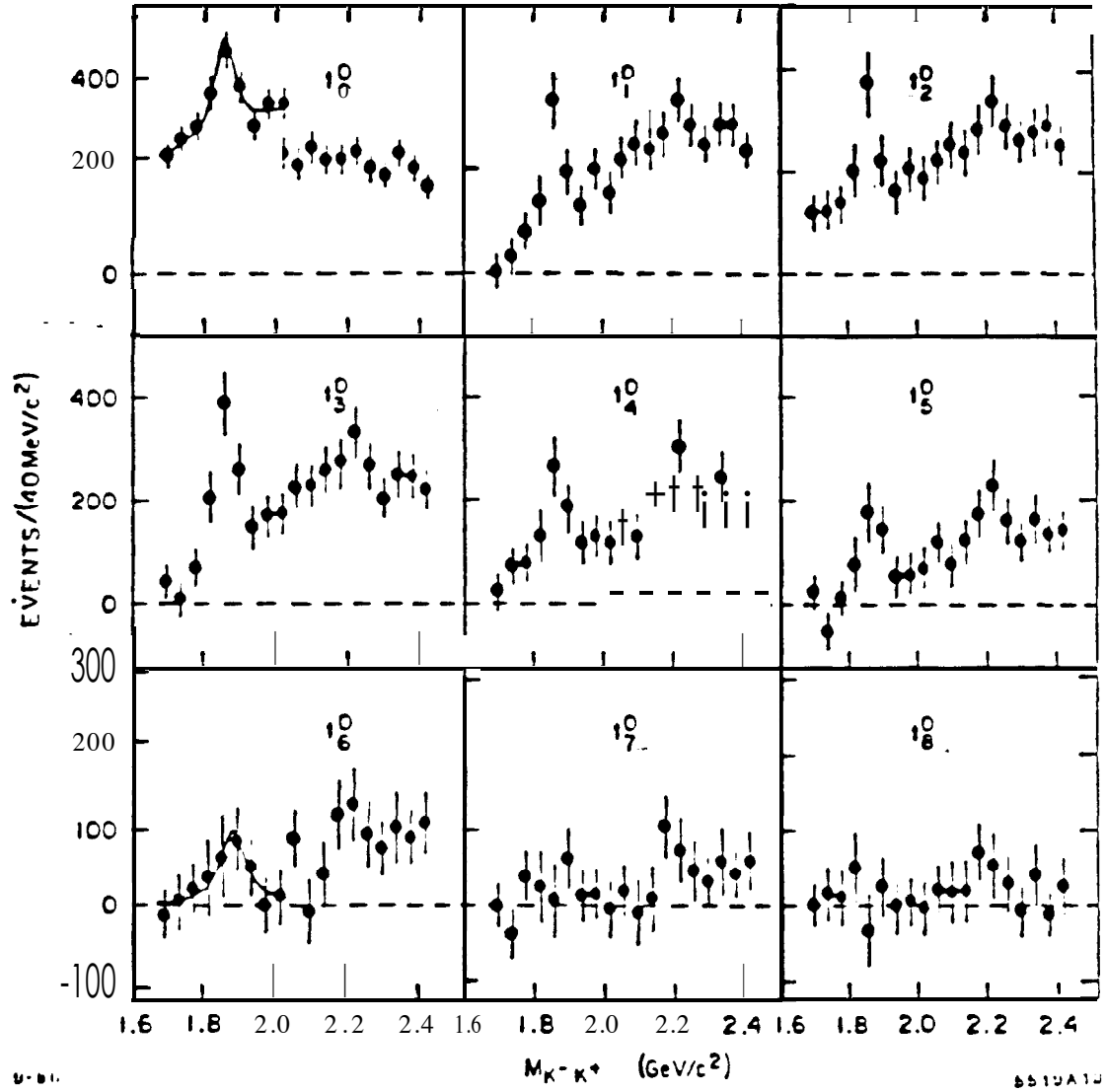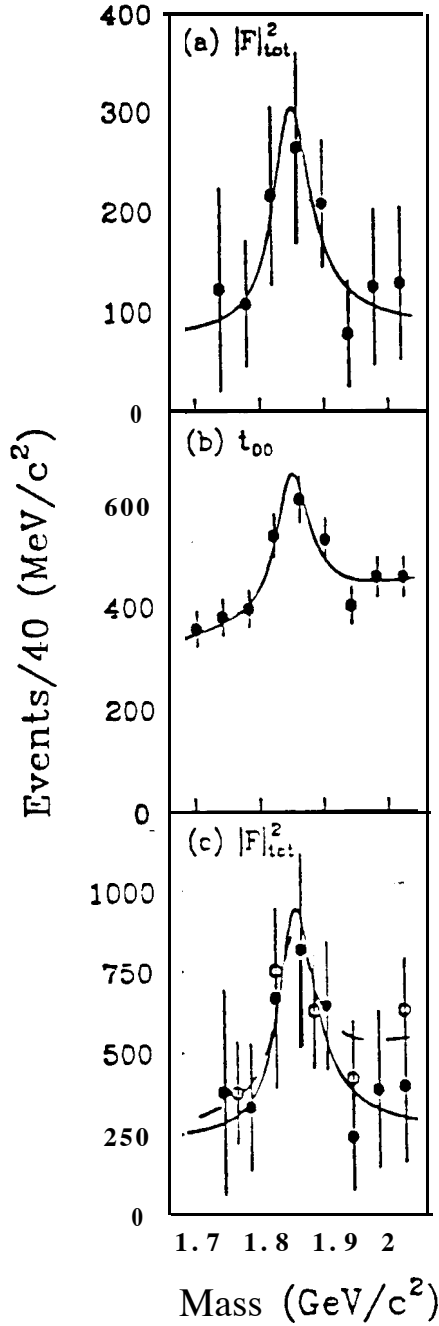
Fig.17. The mass dependence of the unnormalized spherical harmonic moments of the K^-K^+ system from reaction (6) in the region 1.68-2.44 GeV/c^2 and $t' \leq 0.2(GeV/c)^2$.

Fig.18. (a) The total F wave intensity distribution, and (b) the corresponding acceptance-corrected mass distribution from reaction (6) for $t' \leq 1.0(\text{GeV/c})^2$ in the ϕ_3 mass region. (c) The comparison of the F wave intensity distributions, after all corrections, from reaction (6) (solid dots) and reactions (7) (open dots). The curves in (a)-(c) correspond to fits using a BW line shape plus linear background term.
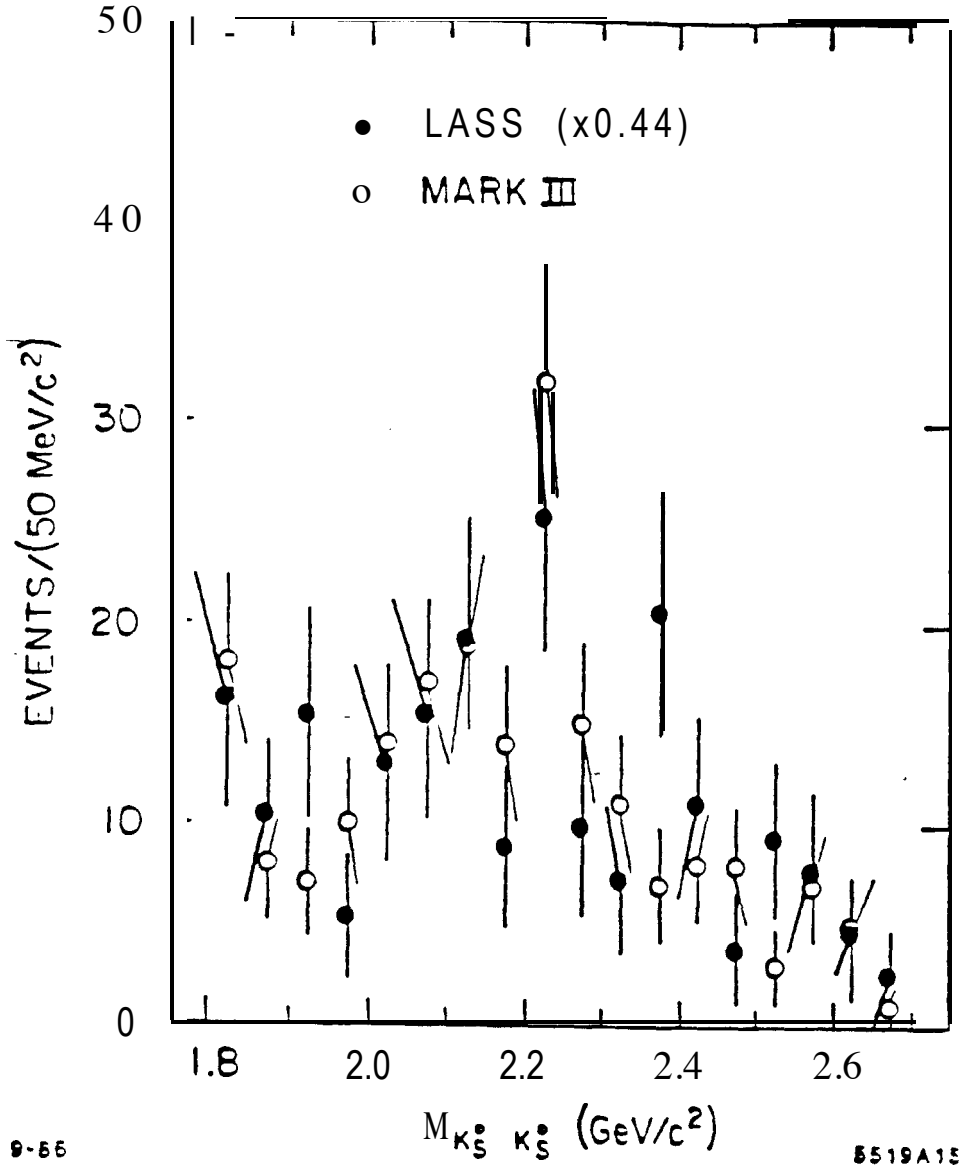
Fig.19. The comparison of the $K_S^0 K_S^0$ mass distribution from reaction (5) with that from radiative J/ψ decay[20] in the mass range 1.8-2.7 GeV/c².
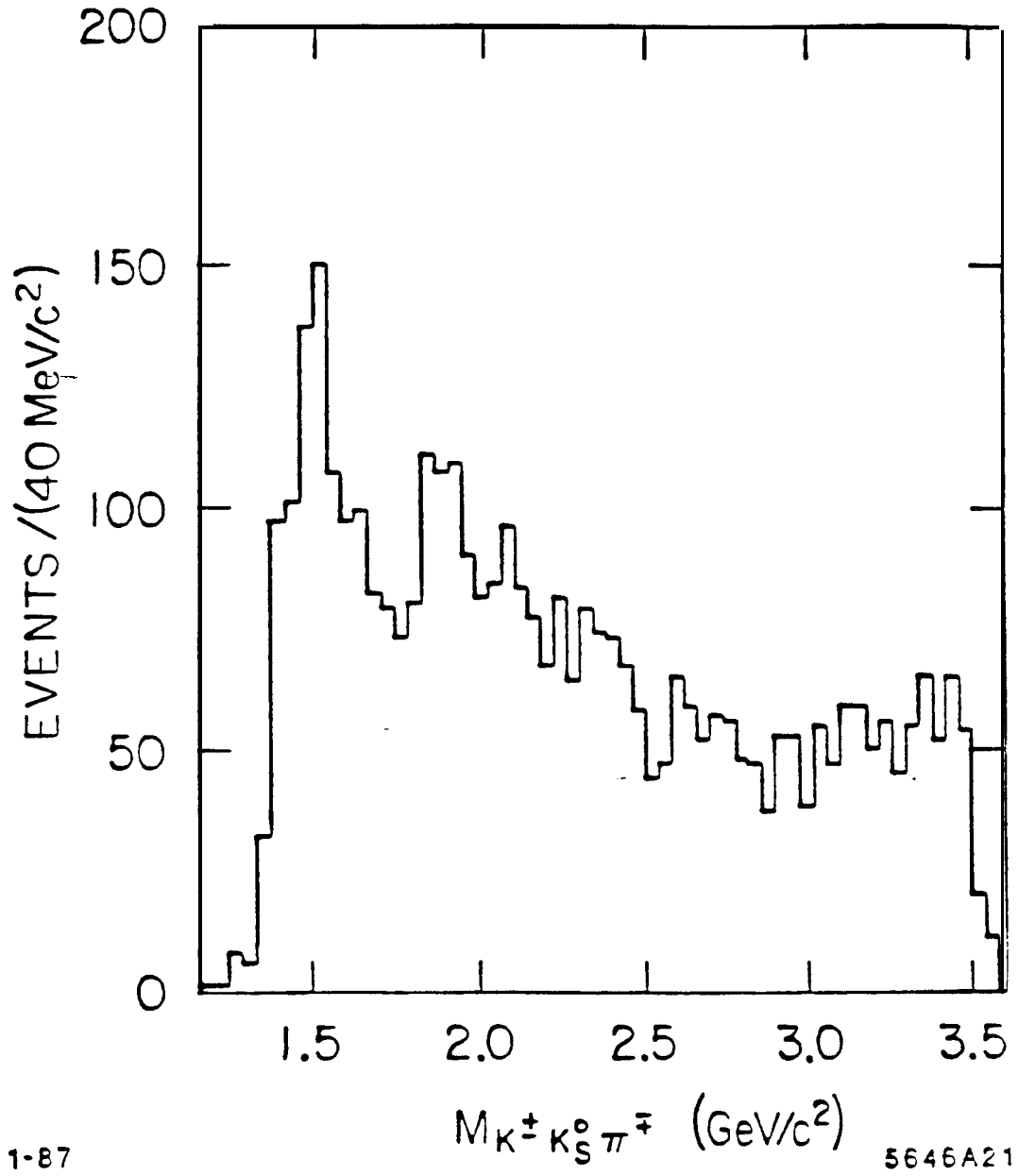
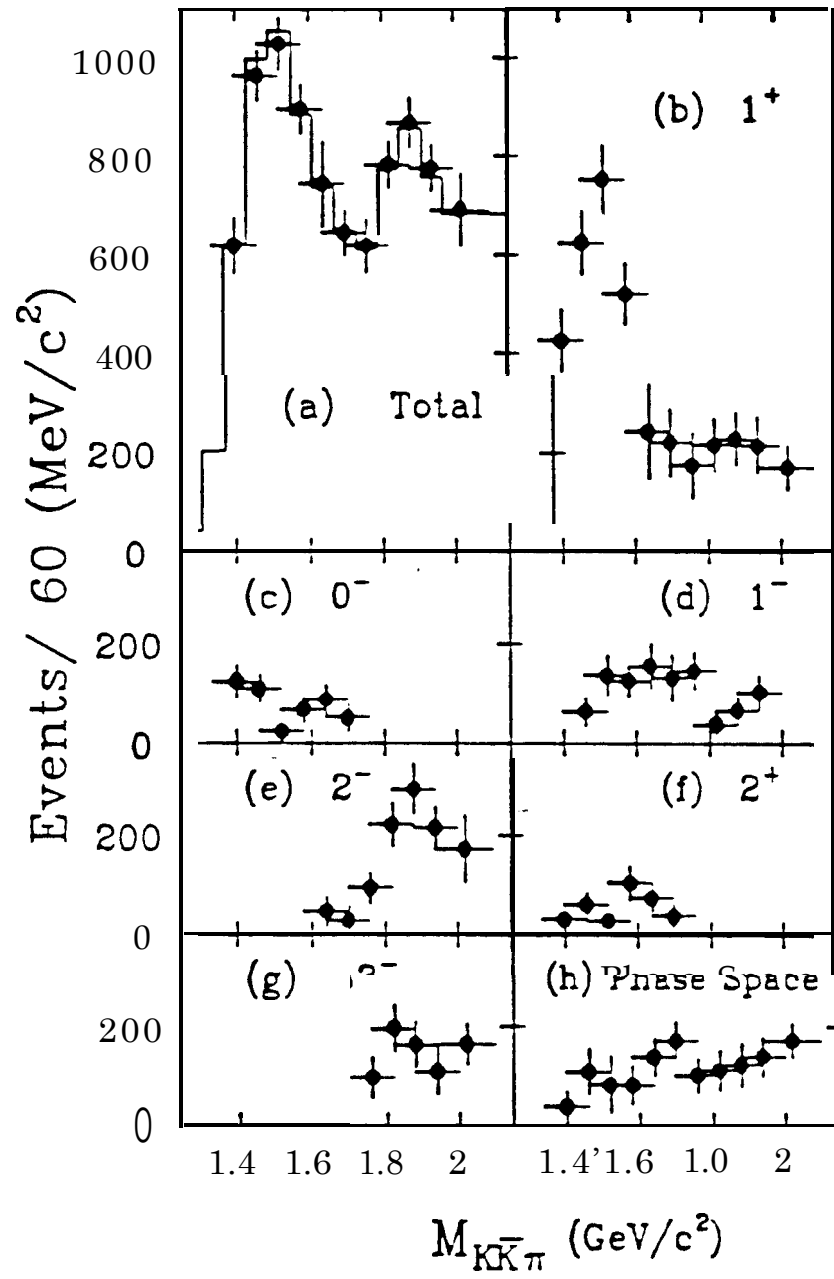Fig.20. The combined raw $K\overline{K}\pi$ mass distributions from reactions (7).

Fig.21. The intensity distributions corresponding to the partial wave decomposition for the $K\overline{K}\pi$ system in reactions (7).
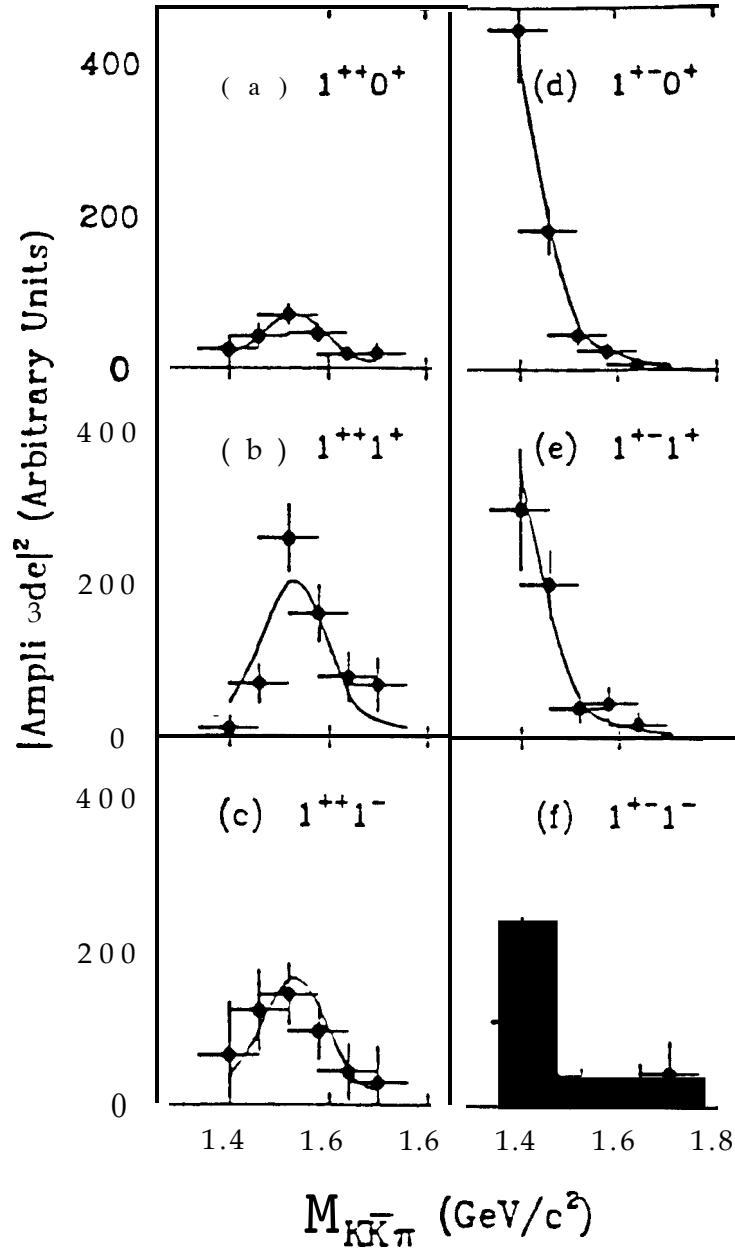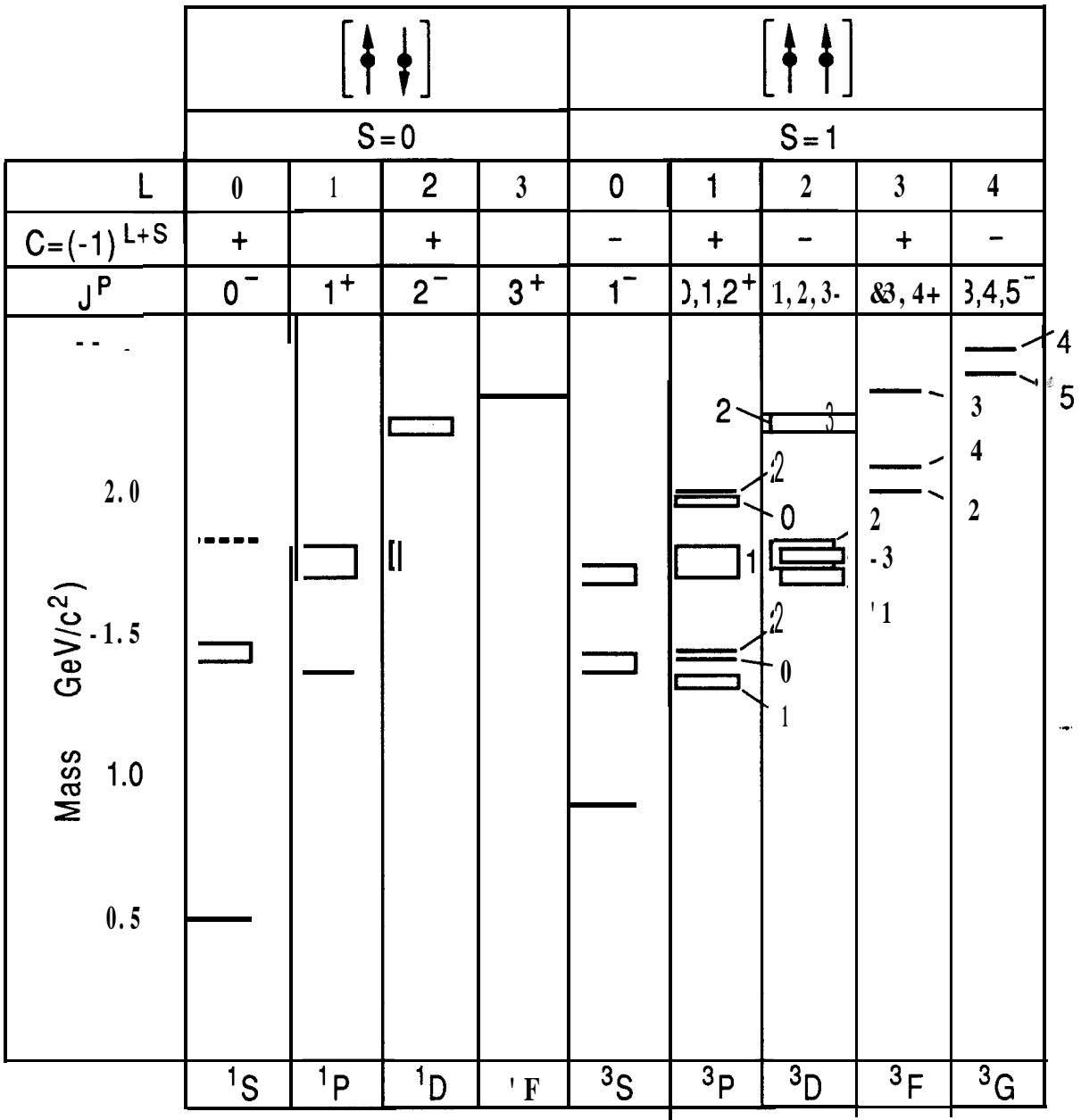
33

Fig.22. The production amplitude intensity distributions from reactions (7) for the $K\overline{K}^*$ and $\overline{K}K^*$ G-parity eigenstate combinations; (a)-(f) are labelled by $J^{PG}M^{\eta}$, where M is the helicity and η the naturality of the t-channel exchange.

34

Strange Meson Level Scheme

	S=0				S=1			
L	0	1	2	3	0	1	2	3	4
$C=(-1)^{L+S}$	+		+		−	+	−	+	−
J^P	0^-	1^+	2^-	3^+	1^-	$0,1,2^+$	$1,2,3-$	$2,3,4+$	$3,4,5^-$

Mass (GeV/c²): 0.5, 1.0, 1.5, 2.0

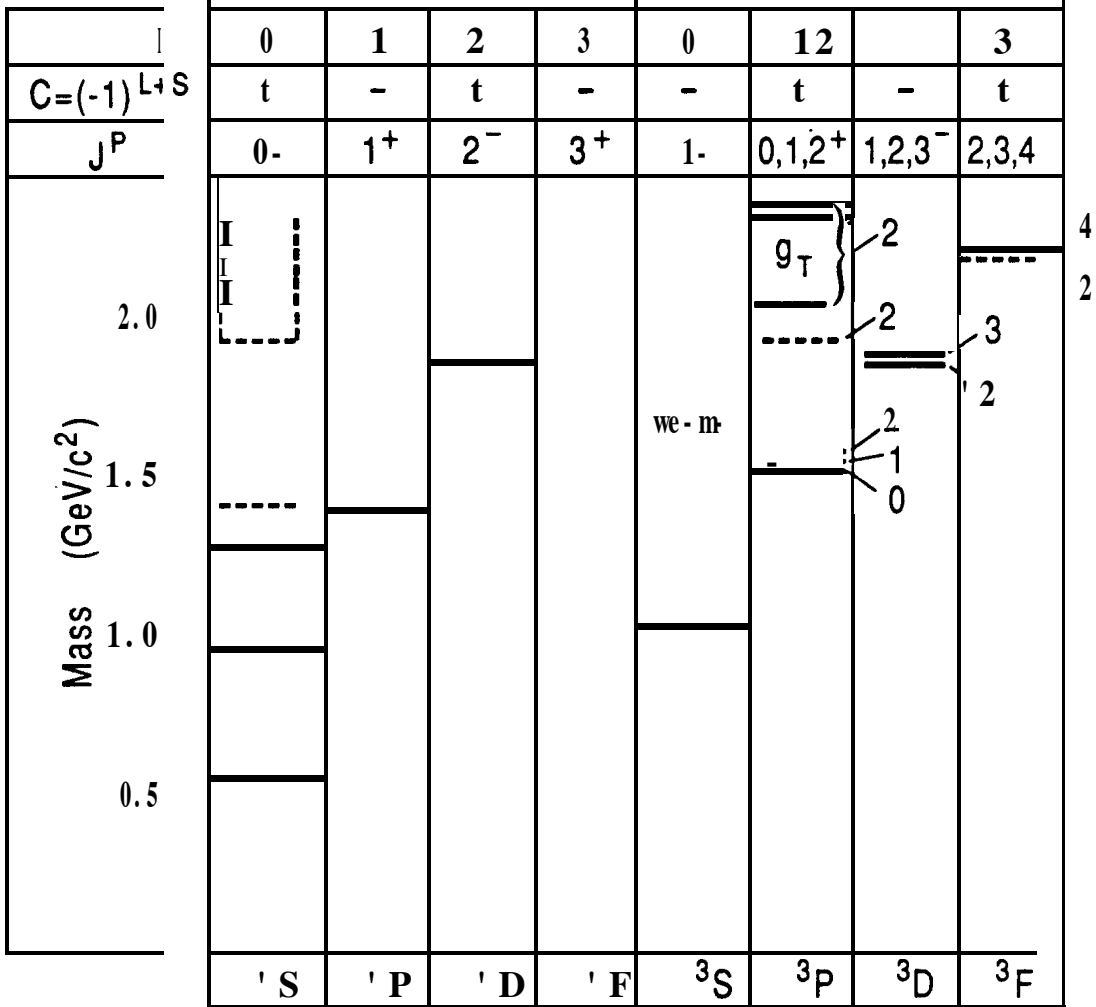^1S ^1P ^1D ^1F ^3S ^3P ^3D ^3F ^3G

4-90

6616A2

Fig.23. The quark model level diagram summarizing the status of strange meson spectroscopy; the C parity is that of the neutral, non-strange members of the relevant SU(3) multiplet.

Mainly s$\bar{\text{s}}$ Level Scheme

Fig.24. The quark model level diagram summarizing the status of the strangeonium states.